Translesion DNA synthesis polymerase kappa functions in the nucleolar stress response

Shilpi Paul[1*], Abbey Rebok[1#], Paolo Cifani[3#], Anirban Paul[2#], Darryl Pappin[3], Tony T. Huang[4], Thomas E. Spratt[1*]

[1]Biochemistry and Molecular Biology, Penn State College of Medicine, Hershey, PA, USA

[2]Neural and Behavioral Sciences, Penn State College of Medicine, Hershey, PA, USA

[3]Cold Spring Harbor Laboratory, Cold Spring Harbor, NY, USA

[4]Biochemistry and Molecular Pharmacology, New York University School of Medicine, NY, USA

# equal contribution

*Corresponding author shilpi@psu.edu and tes13@psu.edu

Abstract

DNA polymerase kappa (Polκ) has multiple cellular roles such as translesion DNA synthesis, replication of repetitive sequences and nucleotide excision repair. Since multiple polymerases are present at the same DNA lesion, by utilizing the selective Polκ substrate, N^2-(4-ethynylbenyl)-2'-deoxyguanosine (EBndG) as bait, isolation of proteins on Pol kappa synthesized DNA (iPoKD) followed by mass-spectrometry captured proteins associated specifically with nascent DNA synthesized with Polκ. We show that, Polκ is active in the nucleolus and Polκ synthesized DNA are enriched with nucleolar proteins. Exposure of cells to benzo[*a*]pyrene diol epoxide (BPDE) increases Polκ stability and induces nucleophosmin 1 translocation to the nucleoplasm, nucleolar cap formation, and reduction in rDNA transcription,

hallmarks of nucleolar stress. The expression and activity of Polκ is regulated by the polycomb complex protein Ring Finger Protein 2 (RNF2) and by the PARylation by poly(ADP)-ribose polymerase 1 (PARP1). This study provides insight into the novel role of Polκ in the nucleolus and in maintaining ribosomal DNA integrity after BPDE damage.

Introduction

DNA polymerase kappa (Polκ) is one of the sixteen DNA-dependent DNA polymerases expressed in humans [1]. The most-studied function of Polκ is translesion DNA synthesis (TLS), which is one of the mechanisms by which the cell responds to DNA damage that cannot be processed by high fidelity DNA polymerases. In this mechanism, Polκ can insert dCMP efficiently opposite bulky N^2-alkyl-dG adducts [2–5]. While the TLS function of Polκ has been the most-studied, other functions of Polκ are being elucidated. Polκ has been linked with nucleotide excision repair [6], cross-link repair [7,8], the production of short oligodeoxynucleotides in the ATR activation pathway and in replication of repetitive DNA sequences [9,10]. A hurdle with determining when and where a specific DNA polymerase is active is that all polymerases utilize undamaged DNA and the four deoxynucleotide triphosphates as substrates. To counter this problem we utilized N^2-4-ethynylbenzyl-2´-deoxyguanosine (EBndG), a non-natural nucleoside that has high specificity for Polκ over other mammalian DNA polymerases [11]. Using this tool, in this study we have identified a role for Polκ in the repair of ribosomal DNA (rDNA).

rDNA is present in the human genome in hundreds of copies. While the 5S rDNA gene is located on chromosome 1, the 5.8S, 18S, and 28S rDNA sequences are located within the

nucleolar organizer regions (NORs) on the short p-arms of chromosomes 13, 14, 15, 21 and 22. Each NOR consists of ~300 repeats of rDNA genes. The rRNA is transcribed as a single transcript to form a 47S pre-rRNA that is processed in the nucleolus before being assembled as the ribosome in the cytoplasm. rDNA is the most actively transcribed regions in the genome and ribosome production comprises the bulk of the energy consumption of the cell [12].

The repetitive nature of the NORs, presence of rDNA genes in clusters on five different chromosomes, high transcription rate that creates conflicts with replication forks [12], altogether leads to replication stress (RS) [13,14]. The transcription-associated R-loops that are formed due to negative supercoiling of DNA behind a transcription bubble, the opening of DNA strands forming stable RNA:DNA hybrids [15,16] are increased under replication stress [17]. Persistent RS and R-loops creates replication fork slowing and stalling, that can lead to long stretches of single-stranded DNA (ssDNA) and single-strand DNA breaks (SSBs). In situations that leads stalled forks to collapse, SSBs converts into double-strand breaks (DSBs). All these together makes the rDNA genes highly vulnerable to DNA damage [18].

Active transcription of rDNA by RNA polymerase I (RNAPI) initiates nucleoli formation, a membrane-less compartment in the nucleus created by liquid-liquid phase separation. The nucleoli are dispersed during mitosis, and with rDNA transcription resuming during telophase small nucleoli around individual NORs are reformed. With progression of cell cycle, nucleoli fuse and forms larger nucleoli containing multiple NORs. The nucleolus is a "tripartite" nuclear structure with sub-compartments, the fibrillar center (FC), the dense fibrillar component (DFC) and the granular component (GC) [19,20]. Transcription of pre-ribosomal RNA (pre-rRNA) occurs at the interface of the FC and DFC compartments. FCs are enriched in components of the RNA Pol I machinery, such as upstream binding transcription factor (UBF1), the fibrillarin

(FBL)-rich DFC contains pre-rRNA processing factors, and the nucleophosmin (NPM1)-rich GC where preribosome subunit assembly occurs.

The nucleolus responds to different types of DNA damaging agents by activating varied signaling pathways leading to activation of ATM and ATR activity that triggers the inhibition of RNA Pol I. This in turn causes dramatic changes in nucleolar structure, protein composition and nucleolar function leading to nucleolar stress [21–24]. One consequence of nucleolar rearrangement is the formation of nucleolar caps in which the FC and the DFC segregate to the exterior of the nucleolus along with rDNA. DNA repair proteins have also been found in the nucleolar caps. It is hypothesized that the localization of repair proteins and damaged DNA aids in the repair of the rDNA [25]. The nature of the DNA damage that causes the nucleolar stress response in not known, as DSBs, acrolein and oxaliplatin induce nucleolar cap formation while cisplatin does not [26–28].

Homologous recombination (HR), non-homologous end joining (NHEJ) and nucleotide excision repair (NER) are found to occur in rDNA. HR proteins are found in nucleolar caps suggesting that HR occurs at these locations while NHEJ proteins are found in the nucleoplasm [23]. Nucleotide excision repair also occurs on rDNA. This repair is inhibited by XPC knockdown indicating that the GG-NER pathway occurs on rDNA. However, CSB knockdown does not reduce NER, indicating that the traditional CSB-dependent TC-NER does not occur in rDNA [29].

The nucleolar DNA damage response is not limited to the repair of rDNA by these pathways. Over 4500 proteins have been found in the nucleolus including 166 DNA repair proteins [30–33]. For instance, almost half of the DNA damage response (DDR) protein poly(ADP)-ribose polymerase 1 (PARP1) is present in the nucleolus [34,35]. Mounting evidences point out nucleolus as a stress response organelle that responds uniquely to different damage and

stressors [36]. Several proteins are released from nucleolus upon nucleolar stress [37,38], such as PARP1 release in the nucleoplasm sensitizes cells to DNA damage-induced apoptosis [35]. NPM1, a chaperone protein that is involved in ribosome biogenesis is also released into the nucleoplasm upon stress where it binds to MDM2 and prevents the MDM2-initiated degradation of p53, leading to the activation of the p53 DDR pathway [39]. Additionally, NPM1 binds to and stabilizes DNA polymerase eta (Polη), increasing its activity in TLS [40].

In this manuscript, we report the role of Polκ in the nucleolar stress response. In response to (+/-)-*trans*-benzo[*a*]pyrene-7,8-dihydrodiol-9,10-epoxide (BPDE) treatment, cells undergo nucleolar stress in which nucleolar caps are formed, NPM1 is translocated from nucleolus to nucleoplasm and the transcription of 47S pre-RNA is inhibited. In spite of the reduced transcription of POLK mRNA, levels of Polκ remain high and enhanced Polκ activity is observed in the nucleolus. The activation of Polκ is dependent on PARP1 PARylation and PRC1 activity.

Results

TLS Polymerase κ (Polκ) is active in the nucleolus

To identify novel cellular roles of Polκ, we took an unbiased proteomics approach to determine the proteins associated with DNA that was replicated with Polκ in cells under normal growth conditions and after exposure to BPDE. We captured the DNA replicated by Polκ by incubating cells with the novel nucleotide analog EBndG, which we showed earlier to be selectively incorporated into DNA by Polκ [11]. We developed a modified aniPOND (accelerated native

isolation of proteins on nascent DNA) [41] procedure, which we called iPoKD (isolation of proteins on Polkappa synthesized DNA) (Paul *et al* manuscript in submission), to capture proteins bound to the nascent DNA synthesized by Polκ. Two different human cell lines (HEK293 and GM12878) were treated with various concentrations of BPDE (low 0.1 μM, medium 0.5 μM, high 2 μM) and subsequently incubated with EBndG, the proteins bound to the DNA containing EBndG were identified by mass spectrometry. To compare the proteins associated with EBndG with proteins present at replication forks and replication-coupled DNA repair mechanisms, we complimented our iPoKD procedure with a traditional aniPOND experiment using BPDE and 5-ethynyl-2'-deoxyuridine (EdU) (Figure 1A).

A Gene Ontology (GO) analysis of our data identified DNA replication and repair proteins (Paul *et al* manuscript in submission) previously identified with EdU pull-downs [42–44]. However, proteins associated with EBndG when compared with EdU pull-downs in both cell lines (Figure 1B, S1A) showed enrichment of nucleolar proteins required for ribosome biogenesis, processing and metabolism (Figure 1C, S1B). Similar enrichment of nucleolar proteins was identified associated with Polκ synthesized DNA in U2OS human osteosarcoma cells using quantitative MS (TMT labelling) after iPoKD. Out of 511 proteins pulled-down with EBndG, 195 are nucleolar residing proteins (Figure S1C). A representation of the subset of the proteins associated with nascent DNA synthesized by Polκ and their fold change compared to the beads control are shown in Figure 1D. Proteins associated with EBndG with and without BPDE damage play roles in rDNA transcription and are present in each of the nucleolar sub-compartments (Figure 1D). The only DNA polymerase that was enriched with the iPoKD technique was Polκ. This observation supports the specificity of EBndG to Polκ and no other polymerase.

BPDE exposure induce nucleolar stress

Since nucleolar proteins are enriched with EBndG pull-down, we questioned whether Polκ is associated with rDNA damage response pathway. To interrogate the novel role of Polκ in the nucleolus, super-resolution microscopy was used to locate and quantify EBndG in U2OS cells. These cells were utilized because they prominently display an average of 6 nucleoli per nucleus [20] and the BPDE treated S-phase arrested cells [45] shows prominent DAPI-less nucleolar cavities. The incorporation of EBndG into DNA was visualized *in situ* by performing the copper(I)-catalyzed azide–alkyne cycloaddition (CuAAC) to covalently label the EBndG with an azide fluorophore. This kind of technique is generally used to visualize 5-EU in nascent RNA [46] or EdU in nascent DNA. EBndG treatment resulted in low levels of incorporation throughout the nucleus with some cells showing nucleolar incorporation (0μM BPDE panels in Figure 2A, B, D and S2A). Following increasing BPDE exposure (0.5 - 2 μM), EBndG incorporation was increased in the nucleus (Figure 2Bii, s2Bii) and become noticeably enriched in the nucleolus compared with the nucleoplasm (Figure 2B, C and D). Treatment with high dose of BPDE (2 μM) resulted in nucleolar EBndG enrichment in all cells (Figure 2C, S2C). This striking observation led us to explore whether BPDE treatment causes nucleolar stress and if Polκ was involved in the DNA damage stress response in the nucleolus.

After treatment with various doses of BPDE (0, 0.1, 0.5 and 2 μM) followed by incubation with EBndG, we examined the localization of NPM1, as its translocation in the nucleoplasm is a typical hallmark of nucleolar stress response [39]. With increasing concentrations of BPDE, NPM1 gradually leaves the nucleolus, initially becoming concentrated on the periphery (Figure

2A) of the nucleolus and then being totally excluded (Figure 2B, C). We also observed an increase in NPM1 protein expression after high dose of BPDE treatment (Figure 2Biii, S2D), and noted that some amount of NPM1 translocation to the cytoplasm in cells treated with high dose of BPDE (Figure 2C, S2C).

We next examined the nucleolar proteins UBF1 and FBL that are present in the FC and DFC, respectively and translocates to nucleolar caps upon nucleolar stress[25]. A significant fraction of BPDE treated cells contained distinct large nucleoli, with rearrangement of UBF1 and FBL proteins to nucleolar caps from the FC and DFC, respectively (Figure 2D, E). We noted that the cells treated with 0.5 μM BPDE have UBF1 foci (Figure S2E), while 2 μM BPDE lead to prominent nucleolar caps with UBF1 outwards and FBL facing inward (Figure 2D and E). Altogether our data suggest that BPDE exposure leads to nucleolar stress.

EBndG is inserted in rDNA and its nuclear incorporation is dependent on Polκ

To confirm that the EBndG incorporation in the nucleus and the nucleolar enrichment observed after BPDE damage is entirely dependent on Polκ, we utilized U2OS sgPolK cells that were previously shown to be deficient in Polκ (Tonzi, Yin et al. 2018). We observed that U2OS sgPolK cells failed to incorporate EBndG in the nucleus or nucleolus (Figure 3A, S3A), and EBndG incorporation was rescued upon complementation with wild-type GFP-POLK (Figure 3B, S3B). We observed that even after 24 hours of treatment, while the wild-type (WT) cells retained EBndG in the nucleolus, there was no trace of nucleolar EBndG in the Polκ deficient cells (Figure S3C). In addition, we used Polκ compromised U2OS cells (siPOLK) (Figure 3Ci, C and D) and observed significantly reduced EBndG incorporation (Figure 3C, 3Cii, S3D). The

POLK transcript level was reduced by ~ 40% in siPOLK cells, that was noticed to be further reduced after BPDE damage (Figure 3D). We observed that the steady state Polκ protein levels were inherently lower in undamaged cells, which was stabilized showing significantly higher level of Polκ upon BPDE damage (Figure 2Bi, S3A). This observation was further confirmed by immunoblot with whole cell protein extracted from these cells and probed with anti-Polκ antibody (Figure 3E). The siPOLK cells (1.3 fold change) showed ~50 % reduction in Polκ protein level after BPDE damage compared to siScrambled RNA transfected cells (2.5 fold change) (Figure 3Ci and E).

In comparison to EBndG enrichment in the nucleolus that is dependent on presence of Polκ in the cell, EdU was incorporated in the entire cell as foci and did not get significantly reduced in Polκ compromised cells (Figure 3F, S3F). We also tested if EBndG incorporation in the nucleolus/nucleus was dependent on any other Y-family members. Cells compromised in Polη, Polι and Rev1 (transfected with respective siRNA pool) showed no reduction in EBndG incorporation (Figure 3G). Instead, we noted an overall increase in EBndG incorporation in Polη compromised cells (Figure 3F graph).

We next queried whether the Polκ dependent EBndG enrichment in the nucleolus is due to the incorporation of EBndG in the rDNA. To test this possibility, we treated the cells with deoxyribonuclease I (DNase I) and observed a significant reduction in total nuclear EBndG intensity and a loss of nucleolar accumulation (Figure 4A, 4B). Upon treatment with RNase A, we observed a small decrease in total nuclear EBndG intensity (Figure 4B) while the nucleolar pattern remained intact (Figure 4A). In contrast, while RNase H treatment did not affect the

total EBndG intensity (Figure 4B), the nucleolar pattern was destroyed (Figure 4A). This result suggested that EBndG is incorporated in rDNA, perhaps in regions containing R-loops.

Polκ cellular expression and nucleolar activity are dependent on PARylation by PARP1

We identified from our iPoKD-MS data that PARP1 is associated with EBndG on DNA newly synthesized by Polκ (Figure 1D). Since approximately 40% of PARP1 molecules reside within nucleoli [35] and DNA-binding of PARP1 induces its catalytic activity, synthesizing poly(ADP)-ribose (PAR) chains on itself, histone and non-histone proteins [47–49] that recruits DDR proteins to the DNA lesions [50]. BPDE treatment induces cellular PAR formation by PARP1 in a time and dose-dependent manner, while inhibition of PARylation by Veliparib (ABT-888) sensitizes cells to BPDE [51].

Since we identified PARP1 on DNA synthesized by Polκ, we hypothesized that the activity of Polκ, especially in rDNA, is dependent on PARP1 PARylation. We inhibited PARylation by PARP1 with olaparib and then damaged the cells with BPDE (high 2μM) followed by incubation with EBndG. We found that olaparib treatment decreased EBndG incorporation both in BPDE-untreated and treated cells (Figure 5B, 5Ci). We also noted that in olaparib-treated cells, Polκ protein expression is significantly reduced (Figure 5B, Cii and D). With combinative treatment of olaparib and BPDE, cells showed excessive stress, as evident by distribution of PARP1 as patches in the cytoplasm indicating that the cells were undergoing apoptosis (Figure 5A).

Recruitment of RNF2 in the periphery of the nucleolus is mediated by PARP1 PARylation and essential for Polκ's nucleolar activity

To understand the mechanism by which PARylation by PARP1 is maintaining the recruitment of Polκ and its activity at the damage sites, we asked whether Polycomb Repressive Complexes (PRCs) proteins have a role in maintaining the activity of Polκ. There are two reasons to examine the involvement of PRCs. First, our iPokD-MS data identified the majority of the PRC canonical proteins including PRC1 protein Ring Finger Protein 2 (RNF2) as being associated with nascent DNA synthesized by Polκ (Figure 1D). Second, it was shown that RNF2 containing complex FBXL10-RNF68-RNF2 ubiquitin ligase complex (FRRUC) recruitment to DNA lesions is mediated by PARP1 and is an early and critical regulatory step in HR [52]. As we predicted, inhibition of PARylation by olaparib significantly reduced RNF2 foci all throughout the nucleus as well as the larger RNF2 discrete foci near nucleolar periphery (Figure 5B, 5Ciii) that possibly are polycomb bodies [53]. It has already been established that PRC proteins play a role in the formation of facultative heterochromatin in the nucleolar-associated domains (NADs) located at the nucleolar periphery [54]. We observed that upon BPDE treatment, large discrete RNF2 bodies are present near the nucleolar periphery compared to the untreated cells (Figure S6A), suggesting the presence of RNF2 in NADs. We observed H2AK119Ub1 to be enriched near nucleolar periphery like RNF2 bodies (Figure S6B), as such it is possible that RNF2 was active at NADs after BPDE damage. This activity is known to be critical for polycomb-mediated transcriptional repression [55].

Since PARP1 PARylation reduced the number of RNF2 containing NADs, we asked whether the nucleolar activity of Polκ is mediated by RNF2 in the NADs. Transfection of cells with siRNF2 significantly reduced RNF2 expression (Figure 6A, Biii, S6C). The RNF2 compromised

cells were untreated or damaged with BPDE followed by incubation with EBndG. Surprisingly, we observed that RNF2 compromised cells have reduced Polκ protein expression (Fig 6A, Bi, and 6C) and these cells failed to incorporate EBndG in the nucleolus and overall nucleus (Figure 6A, 6Bii). Although Polκ protein expression was decreased in RNF2 compromised cells, there was an upregulation of *POLK* transcript (Figure 6D), suggesting that RNF2 transcriptionally inhibits *POLK* gene expression, however these RNF2 knock-down cells fail to maintain the stability of Polκ protein. Altogether, our data suggests that PARP1 PARylation increases the RNF2 foci formation that in turn maintain Polκ activity.

Polκ plays an essential role in recovering from nucleolar stress after BPDE damage

Since our experiments provide evidence that Polκ is active in the nucleolus, we next investigated whether Polκ participates in the recovery of cells from BPDE-induced rDNA damage and nucleolar stress. It was previously shown that persistent S-phase arrest in BPDE (0.1 μM) treated Polκ -/- mouse embryonic fibroblasts (MEFs), lead to DNA double strand breaks (DSBs) as detected by increased levels of γH2AX [56]. In U2OS cells, we observed similar increase in γH2AX in undamaged Polκ compromised cells compared to cells transfected with scrambled siRNA, that profoundly increased after BPDE damage (Figure 7A, S7A). We also noticed γH2AX foci inside and in the periphery of the nucleolus, indicating DSBs in rDNA as shown by the arrows in the +BPDE panels in Figure S7A. Since rDNA damage will hinder rRNA transcription, using RT-qPCR we detected reduced 47S primary pre-rRNA transcript (Figure 7B) in Polκ compromised cells. In addition, we incubated the cells with 5-ethynyluridine (EU) to examine rRNA transcription in the nucleolus. We observed robust

nucleolar EU incorporation in undamaged cells (Figure 7Ci, ii), indicating rRNA transcription. However, after BPDE damage, EU incorporation is significantly reduced in Polκ compromised cells (Figure 7Cii), which becomes more profound in all visible nucleoli after high (2μM) BPDE treatment (Figure 7Ci, S7B). These experiments suggest that Polκ is important for repairing rDNA damage caused by BPDE.

We next examined whether Polκ participates in the recovery from BPDE-induced nucleolar stress. We treated Polκ wild-type and compromised cells with 0.5, or 2 μM BPDE for 2 hours, then fixed the cells immediately (t=2hrs) or left them in growth media to recover for 36 hours (t=36hrs) (schematic in Figure 7D). As observed before (Figure 2A, C), wild-type cells at t=2hrs showed NPM1 translocated from the nucleolus to the nucleoplasm. After 36 hours of recovery, NPM1 returned to the nucleolus and showed enrichment at the nucleolar periphery. However, BPDE treated Polκ compromised cells or deleted, NPM1 redistributed throughout the cell with a majority of NPM1 in the cytoplasm (Figure 7E, S7C). Although in these cells Polκ expression is recovering after 36 hours, the recovery from nucleolar stress is still impaired.

To further examine the role of Polκ in recovering from nucleolar stress, we examined the formation and recovery of nucleolar caps. As illustrated in Figure 7F, treatment of 0.5 μM BPDE lead to the translocation of UBF1 from the interior of the nucleoli to the periphery, an indication of nucleolar cap formation, in both siScrambled and siPOLK cells after 2 hours. After 36 hours, UBF1 returned to the nucleolus in siScrambled cells while Polκ compromised cells retained UBF1 in the nucleolar caps (Figure 7F). This result supports a role of Polκ in the recovery from BPDE-induced nucleolar stress.

As it has been established in BPDE-treated MEFs that Polκ is essential to resume S-phase progression and thus is important for cell survival from BPDE-induced DNA damage [56], we hypothesized that the failure to recover from nucleolar stress in Polκ deficient U2OS cells after BPDE treatment will also hinder cell survival. We performed clonogenic assay with wild-type and sgPolK U2OS (Polk -/-) cells after treatment with BPDE (0, 0.1, 0.5 μM). We noticed that although the number of colonies were only slightly reduced in Polk -/- cells compared to wild-type cells (Figure 7Gi, 7Gii), the area of the colonies were significantly reduced in the Polk -/- cells. We also noticed that the U2OS Polk -/- cells showed significant reduction in colony sizes compared to wild-type cells even without BPDE damage (Figure 7Giii). This result suggests that Polκ deficient cells that survived after 0.1μM BPDE treatment, were slow in recovery from S-phase arrest thus showed reduction in cell proliferation. Similar to MEFs, treatment with 0.5 μM BPDE lead to significant reduction in the number of colonies even in wild-type cells showing BPDE sensitivity. Altogether these data suggest that Polκ deficiency leads to higher BPDE sensitivity and reduction in cell proliferation.

Discussion

We demonstrate that the Y-family TLS polymerase Polκ is active in the nucleolus, and the activity profoundly increases upon BPDE damage, and protects the cell from nucleolar stress. This conclusion relies on two independent experimental approaches. First, by establishing a novel tool, iPoKD-MS, nucleolar proteins were surprisingly discovered to be highly enriched in

DNA that had been synthesized by Polκ. Second, by using super-resolution confocal microscopy, the activity of Polκ in the nucleolus was increased after exposure to BPDE.

Enrichment of PARP1 and the canonical PRC proteins in the iPoKD-MS data, lead us to examine their involvement in Polκ's activity. Our data identified PARylation by PARP1 and the presence of RNF2, the E3 ubiquitin ligase in the PRC1 complex, required to maintain Polκ expression and its activity in the nucleus/nucleolus (Figures 5 and 6). We noted PARP1 in cytoplasm of cells treated with both olaparib and BPDE. This suggests that ablation of PARylation with olaparib lead to inability of cells to respond to BPDE-induced damage by triggering the apoptosis pathway in which the caspase fragmentation of PARP1 produces a smaller PARP1 fragment that translocates to the cytoplasm, and induces apoptosis [57].

Lack of PARylation also reduced RNF2 foci formation. When PARylation is inhibited and RNF2 is down-regulated, the Polκ levels decrease with a consequent decrease in activity. The effect of RNF2 is complex, because siRNF2 cells showed an increased *POLK* transcript but a decreased protein level.

Using the specificity of EBndG for Polκ, we showed that Polκ has activity even in untreated cells (Figure 2). Since Polκ activity is observed in all cells, the activity of Polκ is not cell-cycle dependent and may accompany a DNA repair process. Cells are constantly exposed to endogenous damage [58] and the EBndG incorporation may be related to its NER [6] or cross-link repair [7,8] activity.

The initial damage produced by BPDE is primarily the 10-(deoxyguanosin-N^2-yl)-7,8,9-trihydroxy-7,8,9,10-tetrahydrobenzo[*a*]pyrene (N^2-BP-dG) adduct, but these adducts lead to DSBs as shown by an increase in γH2AX [56,59](Figure 7). BPDE damage induces transcription

arrest at the sites of damage [60] as well as genome-wide [61,62]. We showed that BPDE treatment also induced the nucleolar stress response in the formation of nucleolar caps (Figure 2), the release of NPM1 from the nucleolus into the nucleoplasm (Figure 2), and inhibition of RNAPI transcription of pre 47S rRNA and reduced nucleolar EU incorporation (Figure 7). It is not clear whether the N^2-BP-dG adduct or the induced DSBs lead to the nucleolar stress response.

We found that the level of POLK mRNA was reduced by BPDE damage. However, the Polκ protein level was increased. The half-life of Polκ is 5 hours [63], thus the reduced mRNA levels should lead to lower Polκ levels unless the protein is stabilized. Our finding that the activity of Polκ did not decrease over 36 hours therefore suggests that Polκ protein was stabilized (Figure 7). NPM1 has been shown to regulate TLS by preventing proteasomal degradation of DNA Polη [40]. It is possible that NPM1's upregulation and translocation into the nucleoplasm in BPDE exposed cells helps in maintaining Polκ protein stability, increasing its activity in maintaining genomic stability and thus promoting cell survival. Upon BPDE damage, while the nuclear activity of Polκ increased slightly, there was an increase of the activity of Polκ in the nucleolus as detected by increased EBndG incorporation. We noted that this increase in activity was not due to an increased localization of Polκ to the nucleolus relative to the nucleoplasm (Figure 2), indicating Polκ's role throughout the nucleus including nucleolus.

Treatment with the nuclease DNase I and RNase A indicated that the primary location of the EBndG localization is DNA. The loss of the nucleolar signal with RNase H treatment suggest an association with R-loops in such a manner in which hydrolysis of the RNA allows the EBndG to diffuse throughout the nucleus (Figure 4). R-loops are transient, reversible structures that form in many regions of the genome. Predictors of R-loop presence include

high transcriptional activity, open DNA and high GC content, all present in rDNA [64,65]. R-loops participate in the regulation of transcription, but they also represent a potential source of damage, and their presence must be carefully regulated [66]. The regulation of R-loops depends on RNA-methylation, including METTL3/14 dependent 6-methyladenine (m^6A) and METTL8 dependent 3-methylcytosine formation [67–69]. m^6A RNA was shown to selectively recruit Polκ to UV-damage sites to facilitate repair [70]. Thus, Polκ may interact with nucleolar R-loops.

Down regulation of Polκ resulted in BPDE sensitivity, with apparent increase in DSBs and nucleolar stress. Additionally, the cells with Polκ were able to respond to BPDE-induced nucleolar stress more rapidly than Polκ deficient cells (Figure 7).

In summary, our data suggest that BPDE exposure leads to genomic lesions including rDNA damage that triggers nucleolar stress. During the nucleolar stress response, nucleolar cap forms as foci to repair damaged rDNA, NPM1 expression increased and translocated to the nucleoplasm, potentially enhancing Polκ protein stability and its activity in the DNA repair process. The BPDE-induced DNA lesions induced PARP1 activity that promoted polycomb body formation near nucleolar periphery, which potentially induced facultative heterochromatin regions at the NADs to promote inhibition of rDNA transcription. The activity of Polκ was critical in recovering cells from BPDE-induced nucleolar stress and S-phase arrest. This report provides an understanding of the novel role of Polκ in repairing damaged rDNA and recovering from nucleolar stress opening a new direction and raising several questions, in particular by what mechanism does Polκ play in repair of rDNA, whether NPM1 directly regulates Polκ's stability, and how RNF2 facilitates Polκ protein stability. Since recent evidences connect nucleolar stress as a hallmark in a variety of cancer, neurological and aging-associated

diseases [71,71–73] as well as our data showing Polκ's critical role in nucleolar stress recovery and its involvement in rDNA maintenance, highlights the importance of such mechanistic insights in revealing new therapeutic strategies for multiple disease conditions.

METHODS

Figure 1. EBndG-bound proteins are enriched in the nucleolus, ribosomal biogenesis and in transcriptional repression.

A. Experimental design to identify proteins enriched at nascent DNA synthesized with Polκ captured by EBndG (iPoKD) compared to traditional aniPond. Chemical structures of EdU and EBndG shown.

B. Venn diagrams depicting number of proteins associated with EdU compared to EBndG.

C. GO analysis (ToppGene) of EdU and EBndG-bound unique proteins, shows significantly higher number of nucleolar proteins associated with EBndG compared to EdU that profoundly increases with high (2 μM) dose of BPDE. Gene counts from each pathway is shown in graph and the p-value for each pathway is indicated within each bar. See S1 Table for complete results.

D. Representative list of proteins bound to Polκ synthesized DNA and their fold change compared to the beads control.

Figure 2. BPDE exposure induces nucleolar stress and increases the activity of Polκ in the nucleolus

A. Representative image of cells from *N* = 2 independent experiments showing enrichment of EBndG in the nucleolus and NPM1 enrichment in the nucleolar periphery (shown with arrows) after 0.1 μM BPDE treatment. Cells without BPDE damage also showed incorporation of EBndG in the nucleus and a few cells (as shown) with nucleolar enrichment. U2OS cells were treated with BPDE for 2 hours followed by EBndG for 30 min. Imaging with super resolution confocal microscopy.

B. Total nuclear EBndG intensity significantly increases after 0.5 μM BPDE treatment. Quantitation of cells treated with BPDE (n=47) showed significant increase in total nuclear intensity of (i) EBndG, (ii) NPM1, (iii) Polκ compared to BPDE untreated cells (n=63) and represented as box plots. One representative experiment from two independent experiments is shown. Statistical signifcance was calculated using a one-way analysis of variance and Kruskal-Wallis test: ****P <0.000. Statistical significance calculated using Mann Whitney U test. ****P <0.0001

1. Figure S2B shows graph with more cells analyzed.

C. Representative images of cells from three independent experiments showing that the high dose of BPDE (2 μM) treatment induced EBndG enrichment in the nucleolus, NPM1 expression and translocation from nucleolus to the nucleoplasm. Few cells showing release of some NPM1 in the cytoplasm.

D. Representative images from *N* = 2 independent experiments showing BPDE treatment leads to relocalization of UBF1 from nucleolar FC region to the nucleolar caps (shown by arrows) and EBndG is enriched in the nucleolus.

F. Cells showing post-BPDE treatment FBL relocalizes from DFC nucleolar region to nucleolar caps beneath UBF1 (shown by arrows). All scale bars = 10 μm.

Figure 3: Incorporation of EBndG in the nucleus and nucleolus is dependent on Polκ.

A. Polκ -/- cells showing failure to incorporate EBndG after BPDE damage. The Polκ -/- cells showing slightly higher expression of NPM1 compared to WT U2OS cells. Full image shown in S3A.

B. Expression of WT Polκ in Polκ -/- cells restored the EBndG incorporation into the nucleus and nucleolus (shown by arrows). Images of more cells shown in S3B.

C. EBndG incorporation is reduced in Polκ compromised cells. Nuclear Polκ (i) and EBndG intensity (ii) were quantified between siScrambled (n=80) and siPOLK (n=74) transfected cells and results represented as box plots. Statistical significance calculated using Mann Whitney U test. ****P <0.0001. Images of more cells shown in S3D.

D. POLK transcript is downregulated by BPDE treatment as well as in siPOLK transfected cells. qRT-PCR was used to quantitate the levels of POLK mRNA using GAPDH mRNA as an internal control. Relative expression values were calculated with the comparative CT method (mean ± SEM). All comparisons are relative to siScrambled 0 μM BPDE.

E. Polκ protein expression after BPDE treatment in cells transfected with siPOLK (1.3 FC) is lower compared to siScrambled (siSc) RNA (2.5 FC). Quantification of Polκ bands were performed using vinculin as a loading control. Fold change (FC) were calculated by using Polk

band intensity after normalization with vinculin were compared to siSc without damage. The full blots are shown in Figure SE.

E. EdU incorporation in S phase cells and cells undergoing replication dependent repair is not significantly reduced in Polκ compromised cells. U2OS cells transfected with siPOLK compared to siScrambled RNA were incubated with EdU. Quantitation of intensity were quantified between undamaged cells siScrambled (n=102) and siPOLK (n=103), 2 μM BPDE treated cells siScrambled (n=56) and siPOLK (n=82). Results represented as box plots. Statistical significance was calculated using a one-way analysis of variance and Kruskal-Wallis test. Full image in S3F.

F. EBndG incorporation in cells compromised with Y-family TLS polymerase - siPOLι (n=29), siPOLη (n=46), siREV1(n=49) are not reduced compared to siScrambled transfected cells (n=45). Nucleolar EBndG are shown by arrows. Polη compromised cells instead shows increased uptake of EBndG. Quantitation and statistics as 2E.

****P <0.0001. All scale bars = 10 μm. Full image in S3G.

Figure 4: Nucleolar EBndG is incorporated in nucleolar DNA

Representative image of cells from *N* = 2 independent experiments showing enrichment of EBndG in the nucleolus, Polκ expression and NPM1 enrichment in the nucleoplasm after BPDE exposure followed by treatment with buffer as control (n=177). Cells treated with DNase I (n=214) shows loss of nuclear and nucleolar EBndG, reduced NPM1 and Pol k compared to RNase A (n=203) treatment that retained nucleolar EBndG. RNase H (n=236) treatment

redistributes EBndG throughout the cell. Quantitation and statistical analysis were performed as described in Figure 2B.

Figure 5: Inhibition of PARylation by PARP1 inhibitor olaparib reduced recruitment of RNF2 and decreased the activity of Polκ

A. Representative images from N=2 independent experiments. Cells either treated with DMSO (control) or 10 μM Olaparib (for 3 days) were left undamaged or damaged by 2 μM BPDE. Olaparib treatment does not alter PARP1 expression, however Olaparib treated cells damaged by BPDE shows PARP1 distribution throughout the cell, reduction in EBndG and Polκ.

B. Similar experiment as 5A, cells with olaparib treatment followed by BPDE damage shows reduction in EBndG incorporation, Polκ and RNF2 expression compared to cells treated with DMSO. Magnified images of cells marked by white square are depicted in the last panel.

C. Quantitation of Fig 5B, shows significant reduction in EBndG, Polκ and RNF2 intensity in cells treated with both olaparib and BPDE (n=153) compared to the cells treated with DMSO (n=125). Cells with only Olaparib treatment (n=40) shows reduction in EBndG and RNF2 foci. Statistical analysis as described in Figure2B. All scale bars 10 μm.

D. Cells treated with olaparib as described in Fig 5A shows reduced Polκ protein level (0.1) compared to DMSO control (1.0). Quantitation of the western blot performed with loading control GAPDH.

Figure 6: The activity of Polκ in the nucleolus is associated with peripheral accumulation of Polycomb Protein, Ring Finger Protein 2 (RNF2)

A. Representative images from N= 2 independent experiments showing RNF2 compromised cells have reduced Polκ protein level and EBndG incorporation. Cells were either transfected with siScrambled or siRNF2 RNA, were left undamaged or BPDE damaged followed by incubation with EBndG. Full image in S5A.

B. Quantitation of Fig 5A, shows significant reduction in EBndG, Polκ and RNF2 intensity in cells transfected with siRNF2 (n=184) compared to the cells treated with siScrambled (n=168) after BPDE treatment. Undamaged siRNF2 transfected cells (n=188) also shows reduction in EBndG and Polκ intensity. Statistical analysis as described in Figure2B. All scale bars 10 μm.

C. Protein extracted from cells transfected with siRNF2 (1.1 or 1.2) shows reduced Polκ level compared to siScrambled control cells (1.7). Quantitation of the western blot performed with loading control vinculin.

D. POLK transcript is upregulated in RNF2 compromised cells, however with BPDE treatment POLK is transcriptionally downregulated. qRT-PCR was used to quantitate the levels of POLK mRNA using GAPDH mRNA as an internal control. Relative expression values were calculated with the comparative CT method (mean ± SEM). All comparisons are relative to siScrambled 0 μM BPDE.

Figure 7: Polκ participates in recovering from nucleolar stress after BPDE damage

A. γH2AX is significantly increased in Polκ compromised cells after BPDE damage. Box plot shows the intensity of γH2AX in cells transfected with siScrambled no damage (n=136) or BPDE damage (n=96) and with siPOLK without damage (n=259) or BPDE damage (n=141).

B. Polκ deficiency and BPDE damage leads to less 47S pre-rRNA transcript. qRT-PCR was used to quantitate the levels of 47S pre-rRNA transcript using GAPDH mRNA as an internal control. Relative expression values were calculated with the comparative CT method (mean ± SEM), three technical replicates from N=2. All comparisons are relative to siScrambled.

C. Polκ deficiency and BPDE damage leads to less rRNA transcription (i) EU incorporation is reduced in the nucleolus in cells transfected with siPOLK compared to siScrambled RNA. (ii) Quantification of these cells (n=25-40) treated with 0, 0.1 μM, 0.5 μM BPDE.

D. Experimental design to identify the role of Polκ in BPDE-induced nucleolar stress recovery after 36 hours.

E. Cells transfected with siScrambled (control) shows NPM1 is recovered as shown by enrichment in the nucleolar periphery or some inside the nucleolus after 36 hours. Whereas, cells transfected with siPOLK shows NPM1 released in the cytoplasm. Cells were treated with 0.5 – 2 μM BPDE. Cells transfected with siPOLK after BPDE damage when left for 36 hours shows recovery of Polκ expression.

F. siScrambled (control) or siPOLK transfected cells after BPDE (0.5 μM) treatments shows UBF1 foci formation and accumulation in the nucleolar cap. Control cells shows recovery of UBF1 in the nucleolus after 36 hours whereas the siPOLK transfected cells retains UBF1 in the nucleolar cap. Nucleolar EBndG and UBF1are shown by arrows. All scale bars 10 μm.

G. Colony forming unit assay showing Polκ -/- cells proliferation is reduced and is highly sensitive to BPDE damage compared to WT cells. Colony number and area quantified. Statistical significance calculated on N=6 biological replicates (mean ± SEM).

(1) Vaisman, A.; Woodgate, R. Translesion DNA Polymerases in Eukaryotes: What Makes Them Tick? *Crit Rev Biochem Mol Biol* **2017**, *52* (3), 274–303. https://doi.org/10.1080/10409238.2017.1291576.

(2) Avkin, S.; Goldsmith, M.; Velasco-Miguel, S.; Geacintov, N.; Friedberg, E. C.; Livneh, Z. Quantitative Analysis of Translesion DNA Synthesis across a Benzo[a]Pyrene-Guanine Adduct in Mammalian Cells: THE ROLE OF DNA POLYMERASE κ *. *Journal of Biological Chemistry* **2004**, *279* (51), 53298–53305. https://doi.org/10.1074/jbc.M409155200.

(3) Shachar, S.; Ziv, O.; Avkin, S.; Adar, S.; Wittschieben, J.; Reißner, T.; Chaney, S.; Friedberg, E. C.; Wang, Z.; Carell, T.; Geacintov, N.; Livneh, Z. Two-Polymerase Mechanisms Dictate Error-Free and Error-Prone Translesion DNA Synthesis in Mammals. *EMBO J* **2009**, *28* (4), 383–393. https://doi.org/10.1038/emboj.2008.281.

(4) Jha, V.; Ling, H. Structural Basis for Human DNA Polymerase Kappa to Bypass Cisplatin Intrastrand Cross-Link (Pt-GG) Lesion as an Efficient and Accurate Extender. *J Mol Biol* **2018**, *430* (11), 1577–1589. https://doi.org/10.1016/j.jmb.2018.04.023.

(5) Stern, H. R.; Sefcikova, J.; Chaparro, V. E.; Beuning, P. J. Mammalian DNA Polymerase Kappa Activity and Specificity. **2019**, 20.

(6) Ogi, T.; Lehmann, A. R. The Y-Family DNA Polymerase κ (Pol κ) Functions in Mammalian Nucleotide-Excision Repair. *Nat Cell Biol* **2006**, *8* (6), 640–642. https://doi.org/10.1038/ncb1417.

(7) Minko, I. G.; Yamanaka, K.; Kozekov, I. D.; Kozekova, A.; Indiani, C.; O'Donnell, M. E.; Jiang, Q.; Goodman, M. F.; Rizzo, C. J.; Lloyd, R. S. Replication Bypass of the Acrolein-Mediated Deoxyguanine DNA-Peptide Cross-Links by DNA Polymerases of the DinB Family. *Chem Res Toxicol* **2008**, *21* (10), 1983–1990. https://doi.org/10.1021/tx800174a.

(8) Williams, H. L.; Gottesman, M. E.; Gautier, J. Replication-Independent Repair of DNA Interstrand Crosslinks. *Mol Cell* **2012**, *47* (1), 140–147. https://doi.org/10.1016/j.molcel.2012.05.001.

(9) Baptiste, B. A.; Eckert, K. A. DNA Polymerase Kappa Microsatellite Synthesis: Two Distinct Mechanisms of Slippage-Mediated Errors. *Environmental and Molecular Mutagenesis* **2012**, *53* (9), 787–796. https://doi.org/10.1002/em.21721.

(10) Walsh, E.; Wang, X.; Lee, M. Y.; Eckert, K. A. Mechanism of Replicative DNA Polymerase Delta Pausing and a Potential Role for DNA Polymerase Kappa in Common Fragile Site Replication. *J Mol Biol* **2013**, *425* (2), 232–243. https://doi.org/10.1016/j.jmb.2012.11.016.

(11) Prakasha Gowda, A. S.; Lee, M.; Spratt, T. E. N2-Substituted 2'-Deoxyguanosine Triphosphate Derivatives, Selective Substrates for Human DNA Polymerase κ. *Angew Chem Int Ed Engl* **2017**, *56* (10), 2628–2631. https://doi.org/10.1002/anie.201611607.

(12) Rudra, D.; Warner, J. R. What Better Measure than Ribosome Synthesis? *Genes Dev* **2004**, *18* (20), 2431–2436. https://doi.org/10.1101/gad.1256704.

(13) Gaillard, H.; García-Muse, T.; Aguilera, A. Replication Stress and Cancer. *Nat Rev Cancer* **2015**, *15* (5), 276–289. https://doi.org/10.1038/nrc3916.

(14) Gottipati, P.; Cassel, T. N.; Savolainen, L.; Helleday, T. Transcription-Associated Recombination Is Dependent on Replication in Mammalian Cells. *Mol Cell Biol* **2008**, *28* (1), 154–164. https://doi.org/10.1128/MCB.00816-07.

(15) Aguilera, A.; Gómez-González, B. Genome Instability: A Mechanistic View of Its Causes and Consequences. *Nat Rev Genet* **2008**, *9* (3), 204–217. https://doi.org/10.1038/nrg2268.

(16) Li, X.; Manley, J. L. Cotranscriptional Processes and Their Influence on Genome Stability. *Genes Dev.* **2006**, *20* (14), 1838–1847. https://doi.org/10.1101/gad.1438306.

(17) Gan, W.; Guan, Z.; Liu, J.; Gui, T.; Shen, K.; Manley, J. L.; Li, X. R-Loop-Mediated Genomic Instability Is Caused by Impairment of Replication Fork Progression. *Genes Dev.* **2011**, *25* (19), 2041–2056. https://doi.org/10.1101/gad.17010011.

(18) Lindström, M. S.; Jurada, D.; Bursac, S.; Orsolic, I.; Bartek, J.; Volarevic, S. Nucleolus as an Emerging Hub in Maintenance of Genome Stability and Cancer Pathogenesis. *Oncogene* **2018**, *37* (18), 2351–2366. https://doi.org/10.1038/s41388-017-0121-z.

(19) Pederson, T. The Nucleolus. *Cold Spring Harb Perspect Biol* **2011**, *3* (3), a000638. https://doi.org/10.1101/cshperspect.a000638.

(20) Farley, K. I.; Surovtseva, Y.; Merkel, J.; Baserga, S. J. Determinants of Mammalian Nucleolar Architecture. *Chromosoma* **2015**, *124* (3), 323–331. https://doi.org/10.1007/s00412-015-0507-z.

(21) Kruhlak, M.; Crouch, E. E.; Orlov, M.; Montaño, C.; Gorski, S. A.; Nussenzweig, A.; Misteli, T.; Phair, R. D.; Casellas, R. The ATM Repair Pathway Inhibits RNA Polymerase I Transcription in Response to Chromosome Breaks. *Nature* **2007**, *447* (7145), 730–734. https://doi.org/10.1038/nature05842.

(22) Harding, S. M.; Boiarsky, J. A.; Greenberg, R. A. ATM Dependent Silencing Links Nucleolar Chromatin Reorganization to DNA Damage Recognition. *Cell Rep* **2015**, *13* (2), 251–259. https://doi.org/10.1016/j.celrep.2015.08.085.

(23) van Sluis, M.; McStay, B. A Localized Nucleolar DNA Damage Response Facilitates Recruitment of the Homology-Directed Repair Machinery Independent of Cell Cycle Stage. *Genes Dev* **2015**, *29* (11), 1151–1163. https://doi.org/10.1101/gad.260703.115.

(24) Collins, P. L.; Purman, C.; Porter, S. I.; Nganga, V.; Saini, A.; Hayer, K. E.; Gurewitz, G. L.; Sleckman, B. P.; Bednarski, J. J.; Bassing, C. H.; Oltz, E. M. DNA Double-Strand Breaks Induce H2Ax Phosphorylation Domains in a Contact-Dependent Manner. *Nat Commun* **2020**, *11* (1), 3158. https://doi.org/10.1038/s41467-020-16926-x.

(25) van Sluis, M.; McStay, B. Nucleolar Reorganization in Response to RDNA Damage. *Curr Opin Cell Biol* **2017**, *46*, 81–86. https://doi.org/10.1016/j.ceb.2017.03.004.

(26) Wang, H.; Chen, T.; Weng, C.; Yang, C.; Tang, M. Acrolein Preferentially Damages Nucleolus Eliciting Ribosomal Stress and Apoptosis in Human Cancer Cells. *Oncotarget* **2016**, *7* (49), 80450–80464. https://doi.org/10.18632/oncotarget.12608.

(27) Korsholm, L. M.; Gál, Z.; Nieto, B.; Quevedo, O.; Boukoura, S.; Lund, C. C.; Larsen, D. H. Recent Advances in the Nucleolar Responses to DNA Double-Strand Breaks. *Nucleic Acids Res* **2020**, *48* (17), 9449–9461. https://doi.org/10.1093/nar/gkaa713.

(28) Sutton, E. C.; DeRose, V. J. Early Nucleolar Responses Differentiate Mechanisms of Cell Death Induced by Oxaliplatin and Cisplatin. *J Biol Chem* **2021**, *296*, 100633. https://doi.org/10.1016/j.jbc.2021.100633.

(29) Yang, Y.; Hu, J.; Selby, C. P.; Li, W.; Yimit, A.; Jiang, Y.; Sancar, A. Single-Nucleotide Resolution Analysis of Nucleotide Excision Repair of Ribosomal DNA in Humans and Mice. *Journal of Biological Chemistry* **2019**, *294* (1), 210–217. https://doi.org/10.1074/jbc.RA118.006121.

(30) Ahmad, Y.; Boisvert, F.-M.; Gregor, P.; Cobley, A.; Lamond, A. I. NOPdb: Nucleolar Proteome Database--2008 Update. *Nucleic Acids Res* **2009**, *37* (Database issue), D181-184. https://doi.org/10.1093/nar/gkn804.

(31) Ogawa, L. M.; Baserga, S. J. Crosstalk between the Nucleolus and the DNA Damage Response. *Mol Biosyst* **2017**, *13* (3), 443–455. https://doi.org/10.1039/c6mb00740f.

(32) Moore, H. M.; Bai, B.; Boisvert, F.-M.; Latonen, L.; Rantanen, V.; Simpson, J. C.; Pepperkok, R.; Lamond, A. I.; Laiho, M. Quantitative Proteomics and Dynamic Imaging of the Nucleolus Reveal Distinct Responses to UV and Ionizing Radiation. *Mol Cell Proteomics* **2011**, *10* (10), M111.009241. https://doi.org/10.1074/mcp.M111.009241.

(33) Andersen, J. S.; Lam, Y. W.; Leung, A. K. L.; Ong, S.-E.; Lyon, C. E.; Lamond, A. I.; Mann, M. Nucleolar Proteome Dynamics. *Nature* **2005**, *433* (7021), 77–83. https://doi.org/10.1038/nature03207.

(34) Yung, T. M. C.; Sato, S.; Satoh, M. S. Poly(ADP-Ribosyl)Ation as a DNA Damage-Induced Post-Translational Modification Regulating Poly(ADP-Ribose) Polymerase-1-Topoisomerase I Interaction. *J Biol Chem* **2004**, *279* (38), 39686–39696. https://doi.org/10.1074/jbc.M402729200.

(35) Rancourt, A.; Satoh, M. S. Delocalization of Nucleolar Poly(ADP-Ribose) Polymerase-1 to the Nucleoplasm and Its Novel Link to Cellular Sensitivity to DNA Damage. *DNA Repair (Amst)* **2009**, *8* (3), 286–297. https://doi.org/10.1016/j.dnarep.2008.11.018.

(36) Moore, H. M.; Bai, B.; Boisvert, F.-M.; Latonen, L.; Rantanen, V.; Simpson, J. C.; Pepperkok, R.; Lamond, A. I.; Laiho, M. Quantitative Proteomics and Dynamic Imaging of the Nucleolus Reveal Distinct Responses to UV and Ionizing Radiation. *Mol Cell Proteomics* **2011**, *10* (10), M111.009241. https://doi.org/10.1074/mcp.M111.009241.

(37) Rubbi, C. P.; Milner, J. Disruption of the Nucleolus Mediates Stabilization of P53 in Response to DNA Damage and Other Stresses. *EMBO J* **2003**, *22* (22), 6068–6077. https://doi.org/10.1093/emboj/cdg579.

(38) Xuan, J.; Gitareja, K.; Brajanovski, N.; Sanij, E. Harnessing the Nucleolar DNA Damage Response in Cancer Therapy. *Genes (Basel)* **2021**, *12* (8), 1156. https://doi.org/10.3390/genes12081156.

(39) Boulon, S.; Westman, B. J.; Hutten, S.; Boisvert, F.-M.; Lamond, A. I. The Nucleolus under Stress. *Mol Cell* **2010**, *40* (2), 216–227. https://doi.org/10.1016/j.molcel.2010.09.024.

(40) Ziv, O.; Zeisel, A.; Mirlas-Neisberg, N.; Swain, U.; Nevo, R.; Ben-Chetrit, N.; Martelli, M. P.; Rossi, R.; Schiesser, S.; Canman, C. E.; Carell, T.; Geacintov, N. E.; Falini, B.; Domany, E.; Livneh, Z.

Identification of Novel DNA-Damage Tolerance Genes Reveals Regulation of Translesion DNA Synthesis by Nucleophosmin. *Nat Commun* **2014**, *5* (1), 5437. https://doi.org/10.1038/ncomms6437.

(41) Leung, K. H. T.; El Hassan, M. A.; Bremner, R. A Rapid and Efficient Method to Purify Proteins at Replication Forks under Native Conditions. *BioTechniques* **2013**, *55* (4), 204–206. https://doi.org/10.2144/000114089.

(42) Alabert, C.; Bukowski-Wills, J. C.; Lee, S. B.; Kustatscher, G.; Nakamura, K.; De Lima Alves, F.; Menard, P.; Mejlvang, J.; Rappsilber, J.; Groth, A. Nascent Chromatin Capture Proteomics Determines Chromatin Dynamics during DNA Replication and Identifies Unknown Fork Components. *Nature Cell Biology* **2014**, *16* (3), 281–291. https://doi.org/10.1038/ncb2918.

(43) Dungrawala, H.; Rose, K. L.; Bhat, K. P.; Mohni, K. N.; Glick, G. G.; Couch, F. B.; Cortez, D. The Replication Checkpoint Prevents Two Types of Fork Collapse without Regulating Replisome Stability. *Mol Cell* **2015**, *59* (6), 998–1010. https://doi.org/10.1016/j.molcel.2015.07.030.

(44) Wessel, S. R.; Mohni, K. N.; Luzwick, J. W.; Dungrawala, H.; Cortez, D. Functional Analysis of the Replication Fork Proteome Identifies BET Proteins as PCNA Regulators. *Cell Rep* **2019**, *28* (13), 3497-3509.e4. https://doi.org/10.1016/j.celrep.2019.08.051.

(45) Romagnolo, D.; Jeffy, B.; Samuelson, D.; Payne, C. Microarray Expression Profiles in Breast Cancer MCF-7 Cells Following Exposure to Benzo[a]Pyrene and Its Diol Epoxide. *Nat Genet* **2001**, *27* (4), 83–83. https://doi.org/10.1038/87272.

(46) Gagné, J.-P.; Isabelle, M.; Lo, K. S.; Bourassa, S.; Hendzel, M. J.; Dawson, V. L.; Dawson, T. M.; Poirier, G. G. Proteome-Wide Identification of Poly(ADP-Ribose) Binding Proteins and Poly(ADP-

Ribose)-Associated Protein Complexes. *Nucleic Acids Res* **2008**, *36* (22), 6959–6976. https://doi.org/10.1093/nar/gkn771.

(47) Isabelle, M.; Moreel, X.; Gagné, J.-P.; Rouleau, M.; Ethier, C.; Gagné, P.; Hendzel, M. J.; Poirier, G. G. Investigation of PARP-1, PARP-2, and PARG Interactomes by Affinity-Purification Mass Spectrometry. *Proteome Sci* **2010**, *8*, 22. https://doi.org/10.1186/1477-5956-8-22.

(48) Jungmichel, S.; Rosenthal, F.; Altmeyer, M.; Lukas, J.; Hottiger, M. O.; Nielsen, M. L. Proteome-Wide Identification of Poly(ADP-Ribosyl)Ation Targets in Different Genotoxic Stress Responses. *Mol Cell* **2013**, *52* (2), 272–285. https://doi.org/10.1016/j.molcel.2013.08.026.

(49) Krietsch, J.; Rouleau, M.; Pic, É.; Ethier, C.; Dawson, T. M.; Dawson, V. L.; Masson, J.-Y.; Poirier, G. G.; Gagné, J.-P. Reprogramming Cellular Events by Poly(ADP-Ribose)-Binding Proteins. *Mol Aspects Med* **2013**, *34* (6), 1066–1087. https://doi.org/10.1016/j.mam.2012.12.005.

(50) Fischer, J. M. F.; Zubel, T.; Jander, K.; Fix, J.; Trussina, I. R. E. A.; Gebhard, D.; Bergemann, J.; Bürkle, A.; Mangerich, A. PARP1 Protects from Benzo[a]Pyrene Diol Epoxide-Induced Replication Stress and Mutagenicity. *Arch Toxicol* **2018**, *92* (3), 1323–1340. https://doi.org/10.1007/s00204-017-2115-6.

(51) Rona, G.; Roberti, D.; Yin, Y.; Pagan, J. K.; Homer, H.; Sassani, E.; Zeke, A.; Busino, L.; Rothenberg, E.; Pagano, M. PARP1-Dependent Recruitment of the FBXL10-RNF68-RNF2 Ubiquitin Ligase to Sites of DNA Damage Controls H2A.Z Loading. *eLife* **2018**, *7*, e38771. https://doi.org/10.7554/eLife.38771.

(52) Pirrotta, V.; Li, H.-B. A View of Nuclear Polycomb Bodies. *Curr Opin Genet Dev* **2012**, *22* (2), 101–109. https://doi.org/10.1016/j.gde.2011.11.004.

(53) Bizhanova, A.; Kaufman, P. D. Close to the Edge: Heterochromatin at the Nucleolar and Nuclear Peripheries. *Biochim Biophys Acta Gene Regul Mech* **2021**, *1864* (1), 194666. https://doi.org/10.1016/j.bbagrm.2020.194666.

(54) Tamburri, S.; Lavarone, E.; Fernández-Pérez, D.; Conway, E.; Zanotti, M.; Manganaro, D.; Pasini, D. Histone H2AK119 Mono-Ubiquitination Is Essential for Polycomb-Mediated Transcriptional Repression. *Mol Cell* **2020**, *77* (4), 840-856.e5. https://doi.org/10.1016/j.molcel.2019.11.021.

(55) Bi, X.; Slater, D. M.; Ohmori, H.; Vaziri, C. DNA Polymerase Kappa Is Specifically Required for Recovery from the Benzo[a]Pyrene-Dihydrodiol Epoxide (BPDE)-Induced S-Phase Checkpoint. *J Biol Chem* **2005**, *280* (23), 22343–22355. https://doi.org/10.1074/jbc.M501562200.

(56) Tubbs, A.; Nussenzweig, A. Endogenous DNA Damage as a Source of Genomic Instability in Cancer. *Cell* **2017**, *168* (4), 644–656. https://doi.org/10.1016/j.cell.2017.01.002.

(57) Mattsson, A.; Jernström, B.; Cotgreave, I. A.; Bajak, E. H2AX Phosphorylation in A549 Cells Induced by the Bulky and Stable DNA Adducts of Benzo[a]Pyrene and Dibenzo[a,l]Pyrene Diol Epoxides. *Chem Biol Interact* **2009**, *177* (1), 40–47. https://doi.org/10.1016/j.cbi.2008.09.015.

(58) Tornaletti, S. Transcription Arrest at DNA Damage Sites. *Mutation Research/Fundamental and Molecular Mechanisms of Mutagenesis* **2005**, *577* (1), 131–145. https://doi.org/10.1016/j.mrfmmm.2005.03.014.

(59) Yang, K.; Yang, J.; Yi, J. Nucleolar Stress: Hallmarks, Sensing Mechanism and Diseases. *Cell Stress 2* (6), 125–140. https://doi.org/10.15698/cst2018.06.139.

(60) Weeks, S. E.; Metge, B. J.; Samant, R. S. The Nucleolus: A Central Response Hub for the Stressors That Drive Cancer Progression. *Cell. Mol. Life Sci.* **2019**, *76* (22), 4511–4524. https://doi.org/10.1007/s00018-019-03231-0.

(61) Lafita-Navarro, M. C.; Conacci-Sorrell, M. Nucleolar Stress: From Development to Cancer. *Semin Cell Dev Biol* **2022**, S1084-9521(22)00126-4. https://doi.org/10.1016/j.semcdb.2022.04.001.

(62) Tonzi, P.; Yin, Y.; Lee, C. W. T.; Rothenberg, E.; Huang, T. T. Translesion Polymerase Kappa-Dependent DNA Synthesis Underlies Replication Fork Recovery. *eLife 7*, e41426. https://doi.org/10.7554/eLife.41426.

(63) Lee, S. Y.; Park, J.-H.; Kim, S.; Park, E.-J.; Yun, Y.; Kwon, J. A Proteomics Approach for the Identification of Nucleophosmin and Heterogeneous Nuclear Ribonucleoprotein C1/C2 as Chromatin-Binding Proteins in Response to DNA Double-Strand Breaks. *Biochem J* **2005**, *388* (Pt 1), 7–15. https://doi.org/10.1042/BJ20042033.

(64) Box, J. K.; Paquet, N.; Adams, M. N.; Boucher, D.; Bolderson, E.; O'Byrne, K. J.; Richard, D. J. Nucleophosmin: From Structure and Function to Disease Development. *BMC Molecular Biology* **2016**, *17* (1), 19. https://doi.org/10.1186/s12867-016-0073-9.

(65) Dhar, S. K.; St. Clair, D. K. Nucleophosmin Blocks Mitochondrial Localization of P53 and Apoptosis. *J Biol Chem* **2009**, *284* (24), 16409–16418. https://doi.org/10.1074/jbc.M109.005736.

(66) Mashimo, M.; Onishi, M.; Uno, A.; Tanimichi, A.; Nobeyama, A.; Mori, M.; Yamada, S.; Negi, S.; Bu, X.; Kato, J.; Moss, J.; Sanada, N.; Kizu, R.; Fujii, T. The 89-KDa PARP1 Cleavage Fragment Serves as a

Cytoplasmic PAR Carrier to Induce AIF-Mediated Apoptosis. *J Biol Chem* **2021**, *296*, 100046.

https://doi.org/10.1074/jbc.RA120.014479.

Figure 1. EBndG-bound proteins are enriched in the nucleolus, ribosomal biogenesis and in transcriptional repression.

A. Experimental design to identify proteins enriched at nascent DNA synthesized with Polκ captured by EBndG (iPoKD) compared to traditional aniPond. Chemical structures of EdU and EBndG shown.

B. Venn diagrams depicting number of proteins associated with EdU compared to EBndG.

C. GO analysis (ToppGene) of EdU and EBndG-bound unique proteins, shows significantly higher number of nucleolar proteins associated with EBndG compared to EdU that profoundly increases with high (2 μM) dose of BPDE. Gene counts from each pathway is shown in graph and the p-value for each pathway is indicated within each bar. See S1 Table for complete results.

D. Representative list of proteins bound to Polκ synthesized DNA and their fold change compared to the beads control.

Figure 2. BPDE exposure induces nucleolar stress and increases the activity of Polκ in the nucleolus

A. Representative image of cells from *N* = 2 independent experiments showing enrichment of EBndG in the nucleolus and NPM1 enrichment in the nucleolar periphery (shown with arrows) after BPDE treatment. Cells without BPDE damage also showed incorporation of EBndG in the nucleus and a few cells (as shown) with nucleolar enrichment. U2OS cells were treated with

BPDE for 2 hours followed by EBndG for 30 min. Imaging with super resolution confocal microscopy.

B. Total nuclear EBndG intensity significantly increases after 0.5 μM BPDE treatment. EBndG intensity of cells treated with BPDE 0 μM (n=103), 0.1 μM (n=63) and 0.5 μM (n=148) cells, was measured and represented as box plots. One representative experiment from two independent experiments is shown. Statistical signifcance was calculated using a one-way analysis of variance and Kruskal-Wallis test: ****P <0.0001, *** P=0.0003, ns P=0.0662, when compared to no BPDE.

C. Representative images of cells from three independent experiments showing that the high dose of BPDE (2 μM) treatment induced EBndG enrichment in the nucleolus, NPM1 expression and translocation from nucleolus (shown with arrows) to the nucleoplasm, and upregulation of Polκ compared to BPDE untreated cells .

D. Quantitation of cells treated with 2 μM BPDE (n=194) showed significant increase in total nuclear intensity of (i) EBndG, (ii) NPM1, (iii) Polκ compared to BPDE untreated cells (n=94). Statistical significance calculated using Mann Whitney U test. ****P <0.0001

E. Representative images from *N* = 2 independent experiments showing BPDE treatment leads to relocalization of UBF1 from nucleolar FC region to the nucleolar caps (shown by arrows) and EBndG is enriched in the nucleolus.

F. Cells showing post-BPDE treatment FBL relocalizes from DFC nucleolar region to nucleolar caps beneath UBF1 (shown by arrows). All scale bars = 10 μm.

Figure 3: Incorporation of EBndG in the nucleus and nucleolus is dependent on Polκ.

A. Polκ -/- cells showing failure to incorporate EBndG after BPDE damage. Expression of WT Polκ in Polκ -/- cells restored the EBndG incorporation into the nucleus and nucleolus (shown by arrows). Images of more cells shown in S3.

B. EBndG incorporation is reduced in Pol κ compromised cells. U2OS cells transfected with siPOLK compared to siScrambled RNA. (i) and (ii)Total Pol κ and EBndG intensity were quantified between siScrambled (n=80) and siPOLK (n=74) transfected cells and results represented as box plots. Statistical significance calculated using Mann Whitney U test. ****P <0.0001

C. POLK transcript is downregulated by BPDE treatment as well as in siPOLK transfected cells. qRT-PCR was used to quantitate the levels of POLK mRNA using GAPDH mRNA as an internal control. Relative expression values were calculated with the comparative CT method (mean ± SEM). All comparisons are relative to siScrambled 0 μM BPDE.

D. Polκ protein expression after BPDE treatment in cells transfected with siPOLK (0.9) is lower compared to siScrambled RNA (1.7). Quantification of Polκ bands were performed using vinculin as a loading control.

E. EdU incorporation in S phase cells and cells undergoing replication dependent repair is not significantly reduced in Polκ compromised cells. U2OS cells transfected with siPOLK compared to siScrambled RNA were incubated with EdU. Quantitation of intensity were quantified between undamaged cells siScrambled (n=102) and siPOLK (n=103), 2 μM BPDE treated cells siScrambled (n=56) and siPOLK (n=82). Results represented as box plots. Statistical significance was calculated using a one-way analysis of variance and Kruskal-Wallis test.

F. EBndG incorporation in cells compromised with Y-family TLS polymerase - siPOLι (n=29), siPOLη (n=46), siREV1(n=49) are not reduced compared to siScrambled transfected cells (n=45). Nucleolar EBndG are shown by arrows. Polη compromised cells instead shows increased uptake of EBndG. Quantitation and statistics as 2E.

****P <0.0001. All scale bars = 10 μm.

Figure 4: Nucleolar EBndG is incorporated in nucleolar DNA

Representative image of cells from *N* = 2 independent experiments showing enrichment of EBndG in the nucleolus, Polκ expression and NPM1 enrichment in the nucleoplasm after BPDE exposure followed by treatment with buffer as control (n=177). Cells treated with DNase I (n=214) shows loss of nuclear and nucleolar EBndG, reduced NPM1 and Pol k compared to RNase A (n=203) treatment that retained nucleolar EBndG. RNase H (n=236) treatment redistributes EBndG throughout the cell. Quantitation and statistical analysis were performed as described in Figure 2B.

Figure 5: Inhibition of PARylation by PARP1 inhibitor olaparib reduced recruitment of RNF2 and decreased the activity of Polκ

A. Representative images from N=2 independent experiments. Cells either treated with DMSO (control) or 10 μM Olaparib (for 3 days) were left undamaged or damaged by 2 μM BPDE. Olaparib treatment does not alter PARP1 expression, however Olaparib treated cells damaged by BPDE shows PARP1 distribution throughout the cell, reduction in EBndG and Polκ.

B. Similar experiment as 5A, cells with olaparib treatment followed by BPDE damage shows reduction in EBndG incorporation, Polκ and RNF2 expression compared to cells treated with DMSO. Magnified images of cells marked by white square are depicted in the last panel.

C. Quantitation of Fig 5B, shows significant reduction in EBndG, Polκ and RNF2 intensity in cells treated with both olaparib and BPDE (n=153) compared to the cells treated with DMSO (n=125). Cells with only Olaparib treatment (n=40) shows reduction in EBndG and RNF2 foci. Statistical analysis as described in Figure2B. All scale bars 10 μm.

D. Cells treated with olaparib as described in Fig 5A shows reduced Polκ protein level (0.2) compared to DMSO control (1.0). Quantitation of the western blot performed with loading control GAPDH.

Figure 6: The activity of Polκ in the nucleolus is associated with peripheral accumulation of Polycomb Protein, Ring Finger Protein 2 (RNF2)

A. Representative images from N= 2 independent experiments showing RNF2 compromised cells have reduced Polκ protein level and EBndG incorporation. Cells were either transfected with siScrambled or siRNF2 RNA, were left undamaged or BPDE damaged followed by incubation with EBndG.

B. Quantitation of Fig 5A, shows significant reduction in EBndG, Polκ and RNF2 intensity in cells transfected with siRNF2 (n=184) compared to the cells treated with siScrambled (n=168) after BPDE treatment. Undamaged siRNF2 transfected cells (n=188) also shows reduction in EBndG and Polκ intensity. Statistical analysis as described in Figure2B. All scale bars 10 μm.

C. Protein extracted from cells transfected with siRNF2 (1.1 or 1.2) shows reduced Polκ level compared to siScrambled control cells (1.7). Quantitation of the western blot performed with loading control vinculin.

D. POLK transcript is upregulated in RNF2 compromised cells, however with BPDE treatment POLK is transcriptionally downregulated. qRT-PCR was used to quantitate the levels of POLK mRNA using GAPDH mRNA as an internal control. Relative expression values were calculated with the comparative CT method (mean ± SEM). All comparisons are relative to siScrambled 0 μM BPDE.

Figure 7: Polκ participates in recovering from nucleolar stress after BPDE damage

A. γH2AX is significantly increased in Polκ compromised cells after BPDE damage. Box plot shows the intensity of γH2AX in cells transfected with siScrambled no damage (n=136) or BPDE damage (n=96) and with siPOLK without damage (n=259) or BPDE damage (n=141).

B. Polκ deficiency and BPDE damage leads to less 47S pre-rRNA transcript. qRT-PCR was used to quantitate the levels of 47S pre-rRNA transcript using GAPDH mRNA as an internal control. Relative expression values were calculated with the comparative CT method (mean ± SEM), three technical replicates from N=2. All comparisons are relative to siScrambled.

C. Polκ deficiency and BPDE damage leads to less rRNA transcription (i) EU incorporation is reduced in the nucleolus in cells transfected with siPolk compared to siScrambled RNA. (ii) Quantification of these cells (n=25-40) treated with 0, 0.1 μM, 0.5 μM BPDE.

D. Experimental design to identify the role of Polκ in BPDE-induced nucleolar stress recovery after 36 hours.

E. Cells transfected with siScrambled (control) shows NPM1 is recovered as shown by enrichment in the nucleolar periphery or some inside the nucleolus after 36 hours. Whereas, cells transfected with siPOLK shows NPM1 released in the cytoplasm. Cells were treated with 0.5 – 2 μM BPDE. Cells transfected with siPOLK after BPDE damage when left for 36 hours shows recovery of Polκ expression.

F. siScrambled (control) or siPOLK transfected cells after BPDE (0.5 μM) treatments shows UBF1 foci formation and accumulation in the nucleolar cap. Control cells shows recovery of UBF1 in the nucleolus after 36 hours whereas the siPOLK transfected cells retains UBF1 in the nucleolar cap. Nucleolar EBndG and UBF1are shown by arrows. All scale bars 10 μm.

G. Colony forming unit assay showing Polκ -/- cells proliferation is reduced and is highly sensitive to BPDE damage compared to WT cells. Colony number and area quantified. Statistical significance calculated on N=6 biological replicates (mean ± SEM).

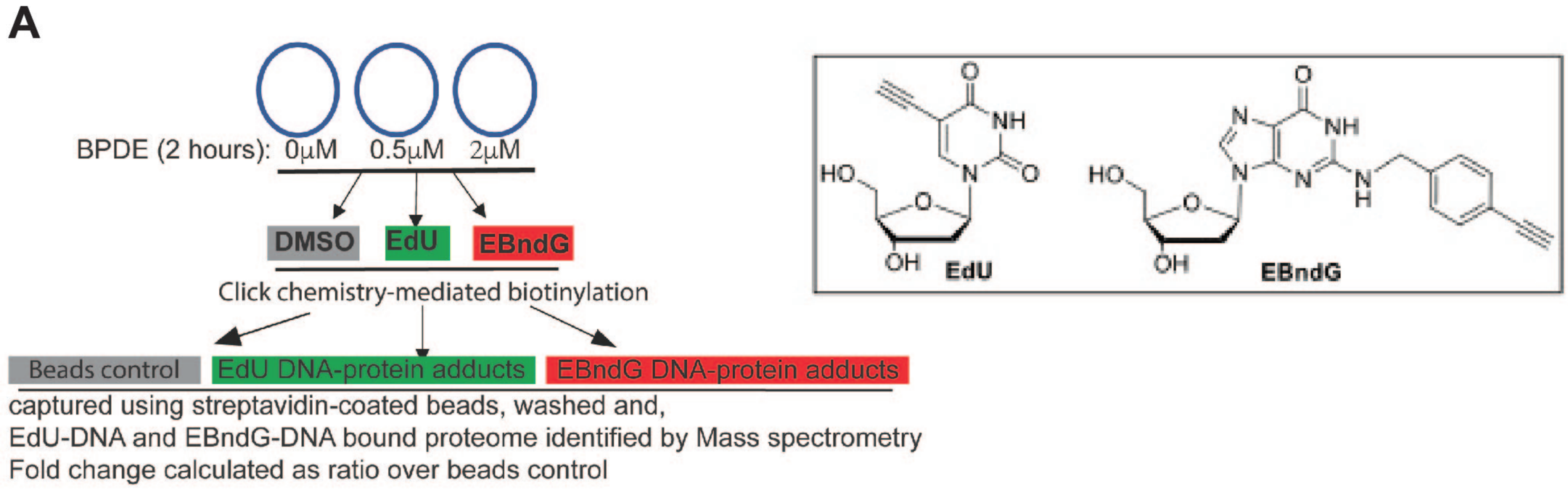

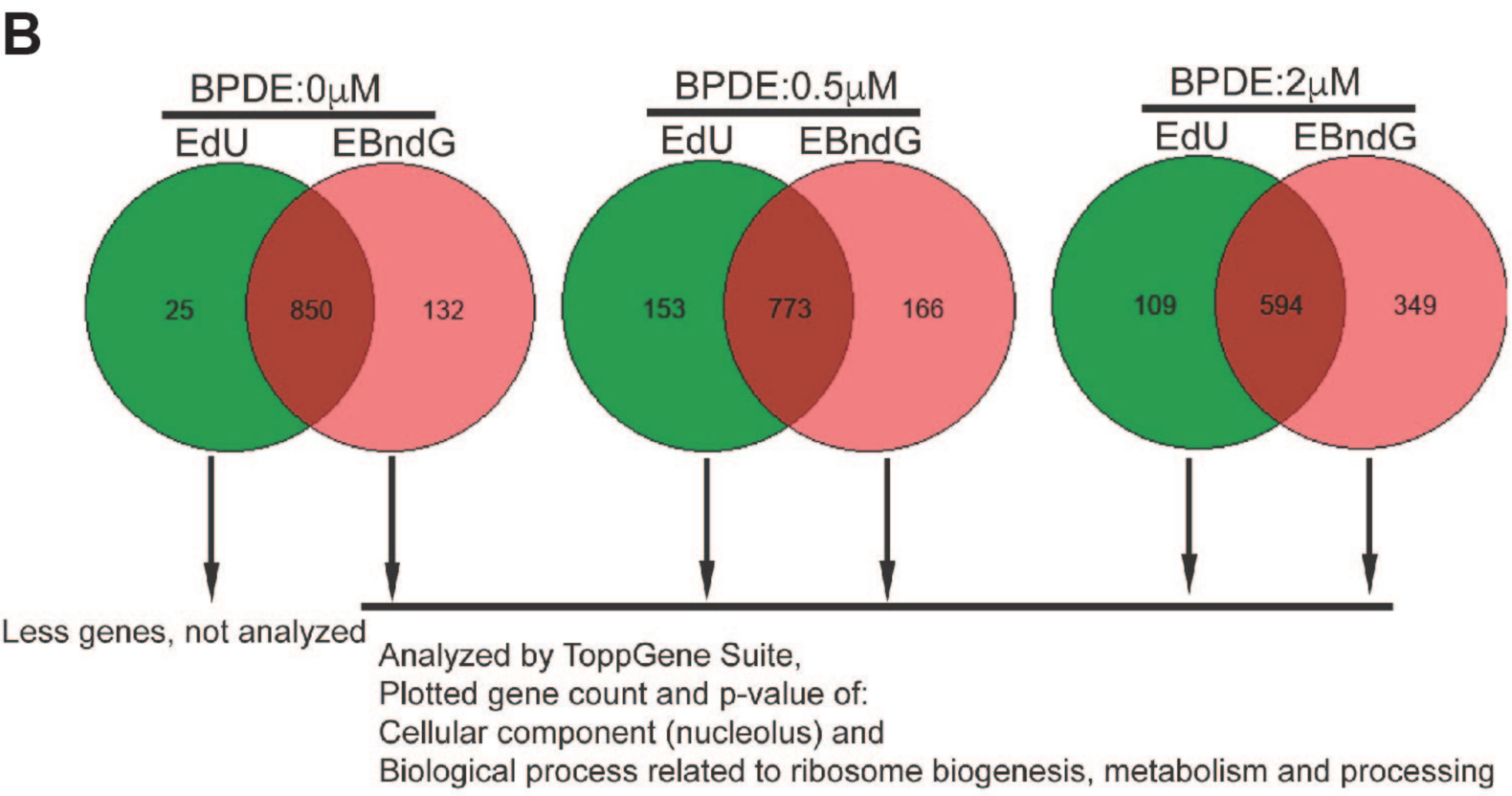

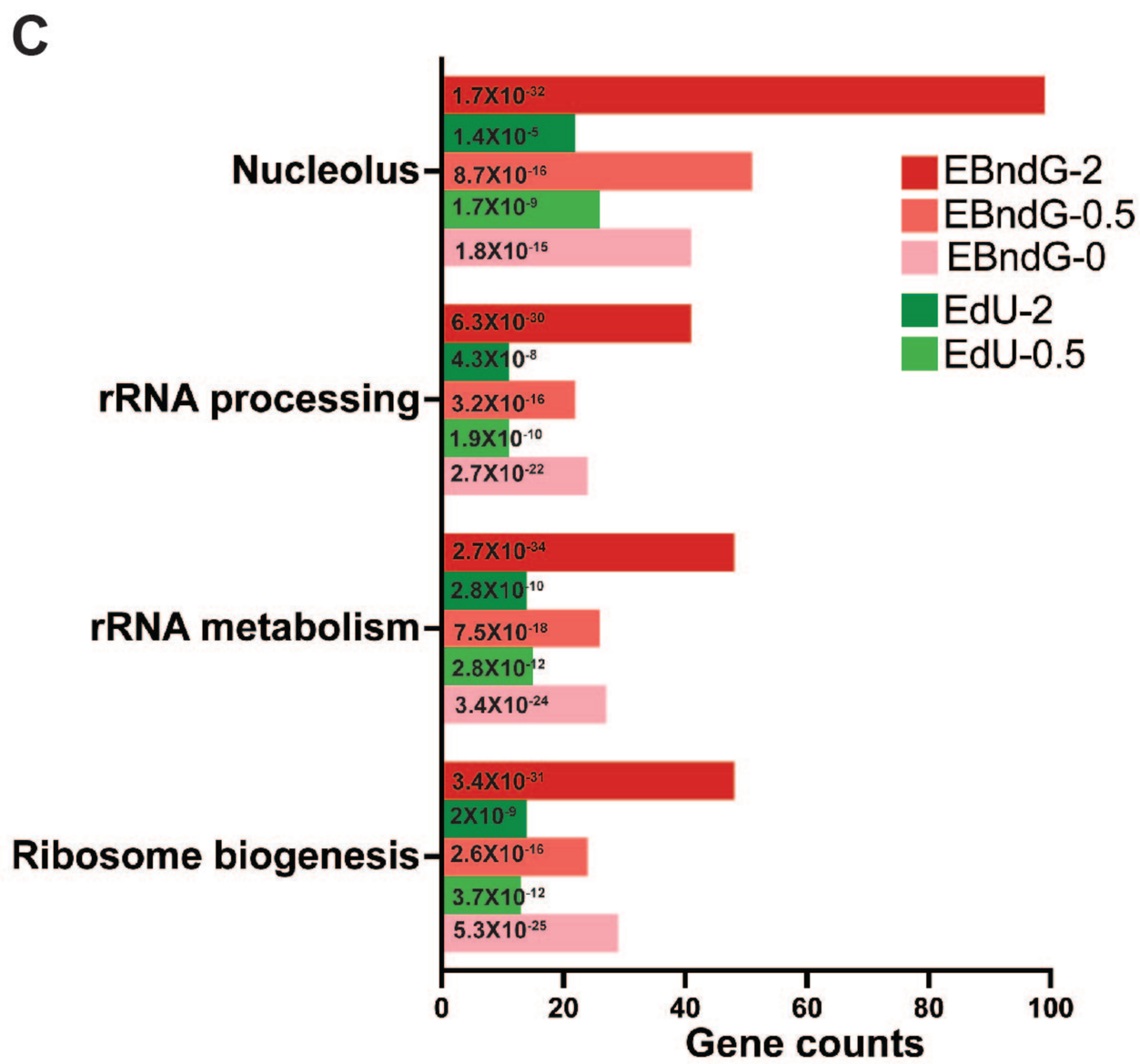

D

	GM12878			HEK293	
Symbol	0μM*	0.5μM *	2μM *	2μM *	
BOP1	9.5	7.7	8	8.4	PeBoW complex
PES1	11.8	10.6	11.4	8.5	
WDR12	9.2	7.6	7.7	3.4	
NPM1	6.8	5.7	6	7	GC FC DFC
UBTF	16	15.4	16.4	11	
FBL	13.6	12	12.4	12.8	
TCOF1	2	0	1.7	6.8	
POLR1B	3	4.4	4.4	4.6	RNA Pol I
POLR1A	9.3	8.5	8.5	8.8	
PARP1	7.2	6	6.7	5.4	
RNF2	4.2	3.8	6.8	7.2	PRC
CBX8	6.3	4.3	5.6	8.6	
SUZ12	7.2	6.1	6.4	6	
EED	7.2	6	6.8	5.6	
POLK	6.9	5.4	6.7	3	

* BPDE concentration

FIGURE1

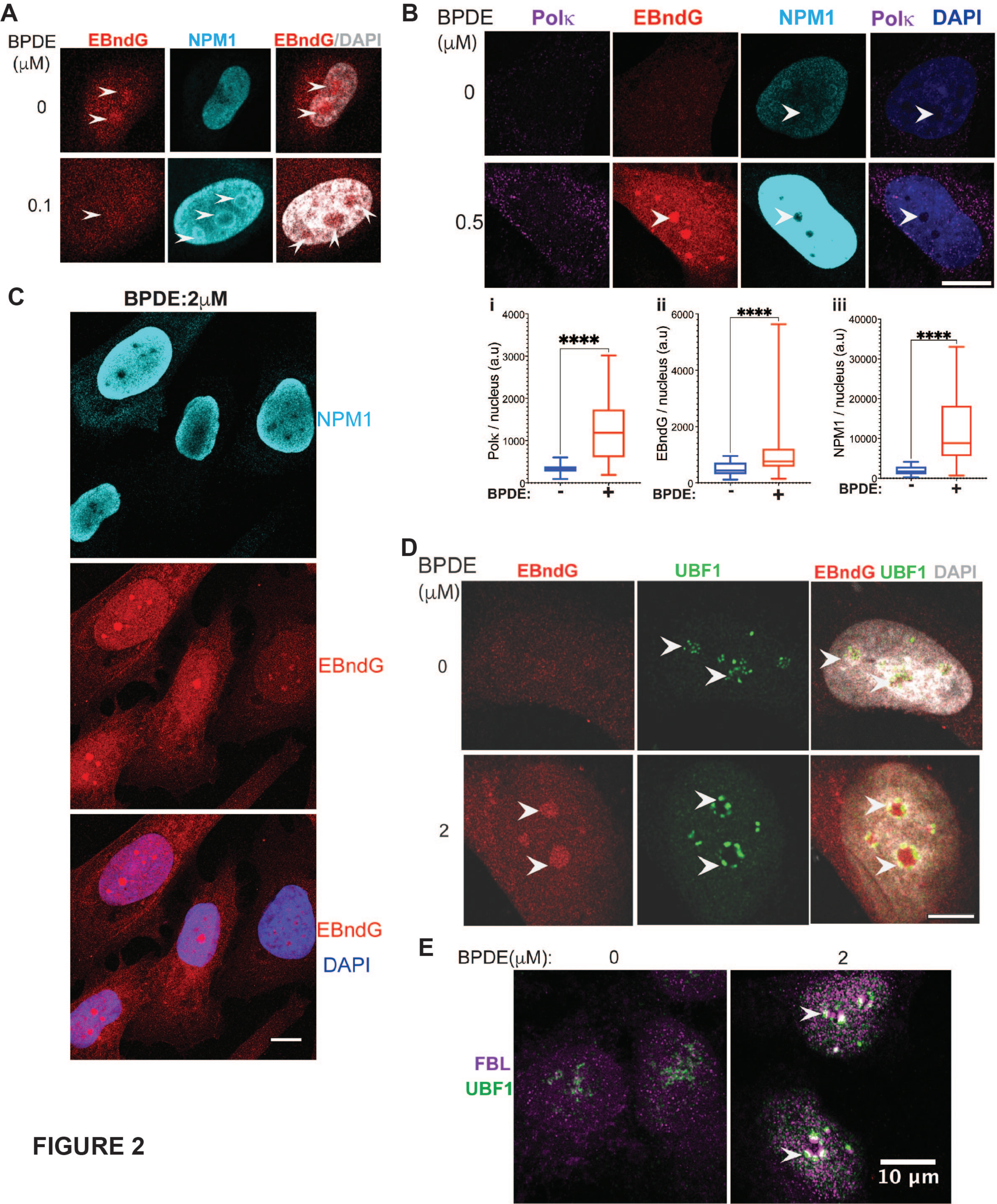
A
BPDE (μM)
EBndG
NPM1
EBndG/DAPI
0
0.1
B
BPDE (μM)
Polκ
EBndG
NPM1
Polκ DAPI
0
0.5
i
ii
iii
Polk / nucleus (a.u)
EBndG / nucleus (a.u)
NPM1 / nucleus (a.u)
****
BPDE:
-
+
C
BPDE:2μM
NPM1
EBndG
EBndG
DAPI
D
BPDE (μM)
EBndG
UBF1
EBndG UBF1 DAPI
0
2
E
BPDE(μM):
0
2
FBL
UBF1
10 μm

FIGURE 2

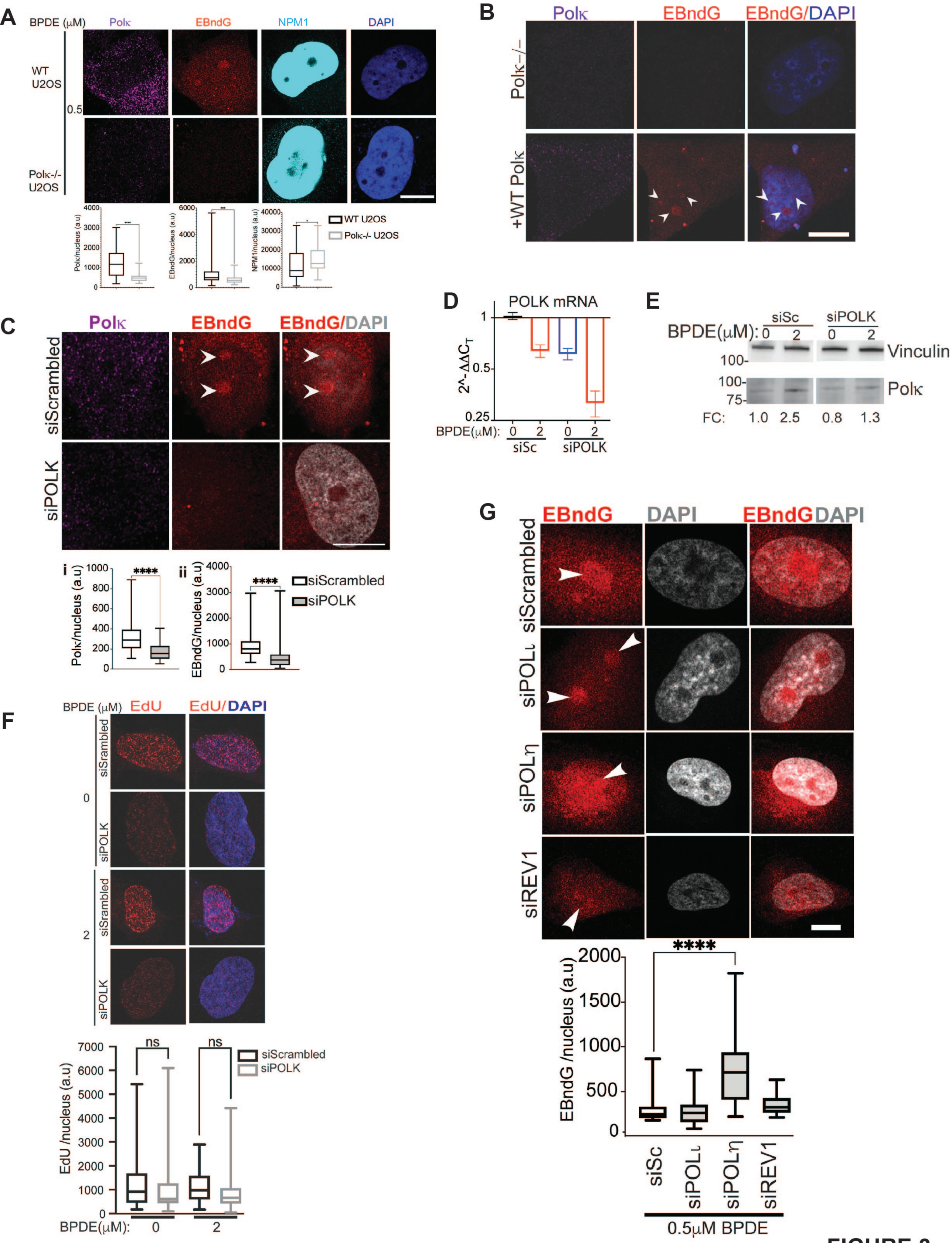
A
BPDE (μM)
Polκ
EBndG
NPM1
DAPI
WT U2OS
0.5
Polκ-/- U2OS
Polκ/nucleus (a.u)
EBndG/nucleus (a.u)
NPM1/nucleus (a.u)
WT U2OS
Polκ-/- U2OS
B
Polκ
EBndG
EBndG/DAPI
Polκ-/-
+WT Polκ
C
Polκ
EBndG
EBndG/DAPI
siScrambled
siPOLK
i
ii
Polκ/nucleus (a.u)
EBndG/nucleus (a.u)
****
siScrambled
siPOLK
D
POLK mRNA
2^-ΔΔC_T
BPDE(μM): 0 2 0 2
siSc
siPOLK
E
siSc
siPOLK
BPDE(μM): 0 2 0 2
Vinculin
Polκ
FC: 1.0 2.5 0.8 1.3
F
BPDE (μM)
EdU
EdU/DAPI
siSrambled
siPOLK
0
2
ns
EdU /nucleus (a.u)
siScrambled
siPOLK
BPDE(μM): 0 2
G
EBndG
DAPI
EBndG DAPI
siScrambled
siPOLι
siPOLη
siREV1
****
EBndG /nucleus (a.u)
siSc
siPOLι
siPOLη
siREV1
0.5μM BPDE

FIGURE 3

FIGURE 4

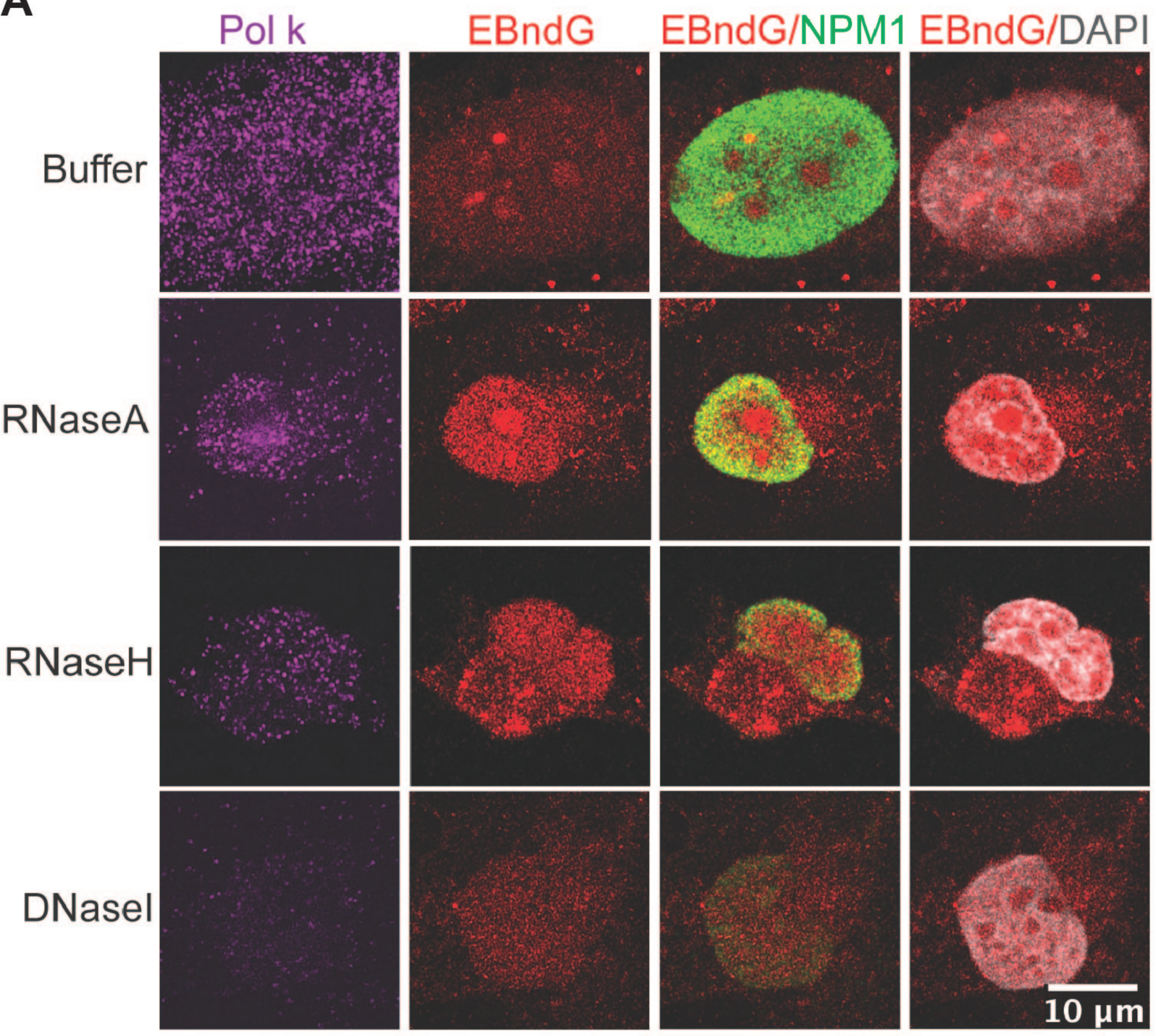

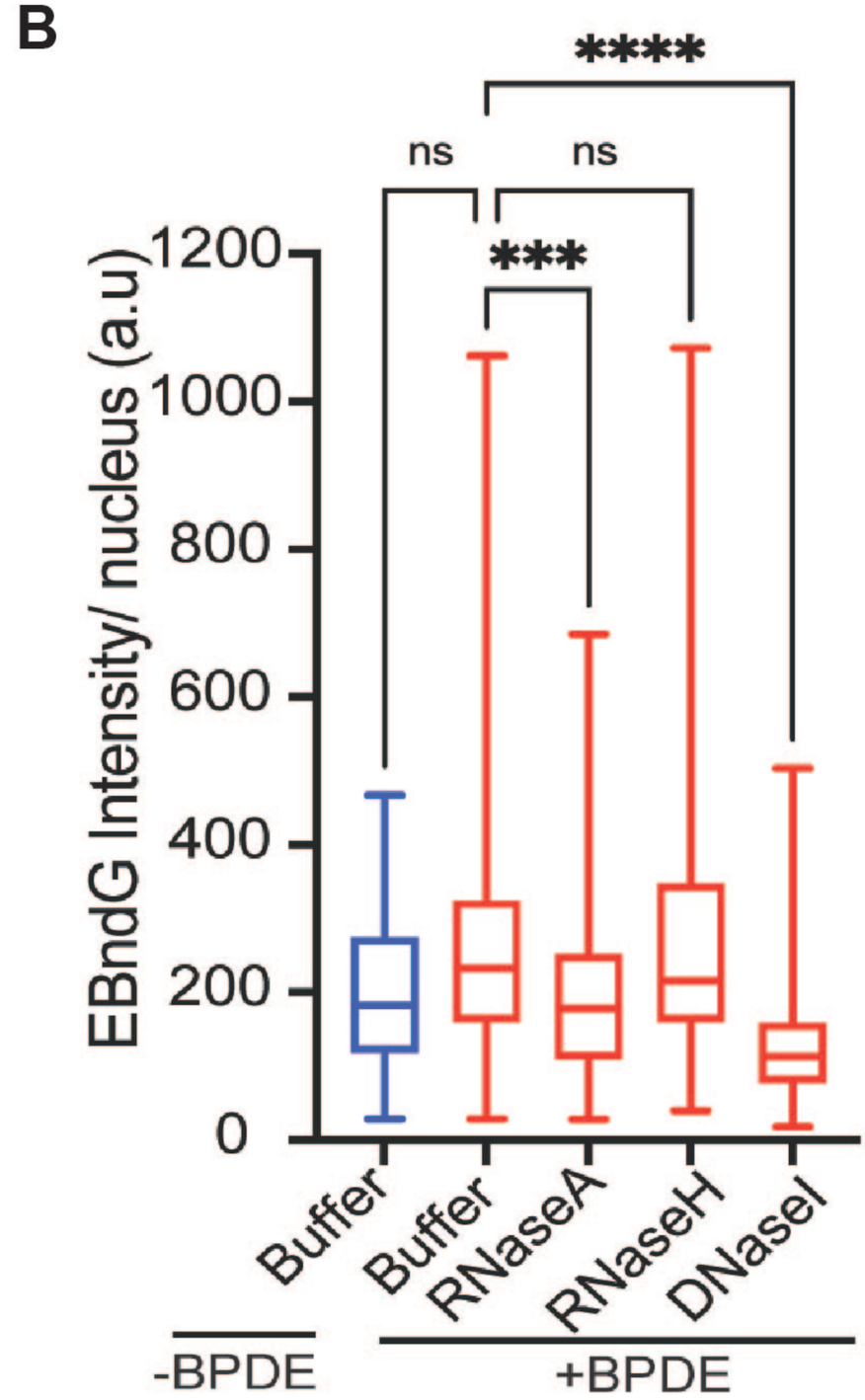

FIGURE 4

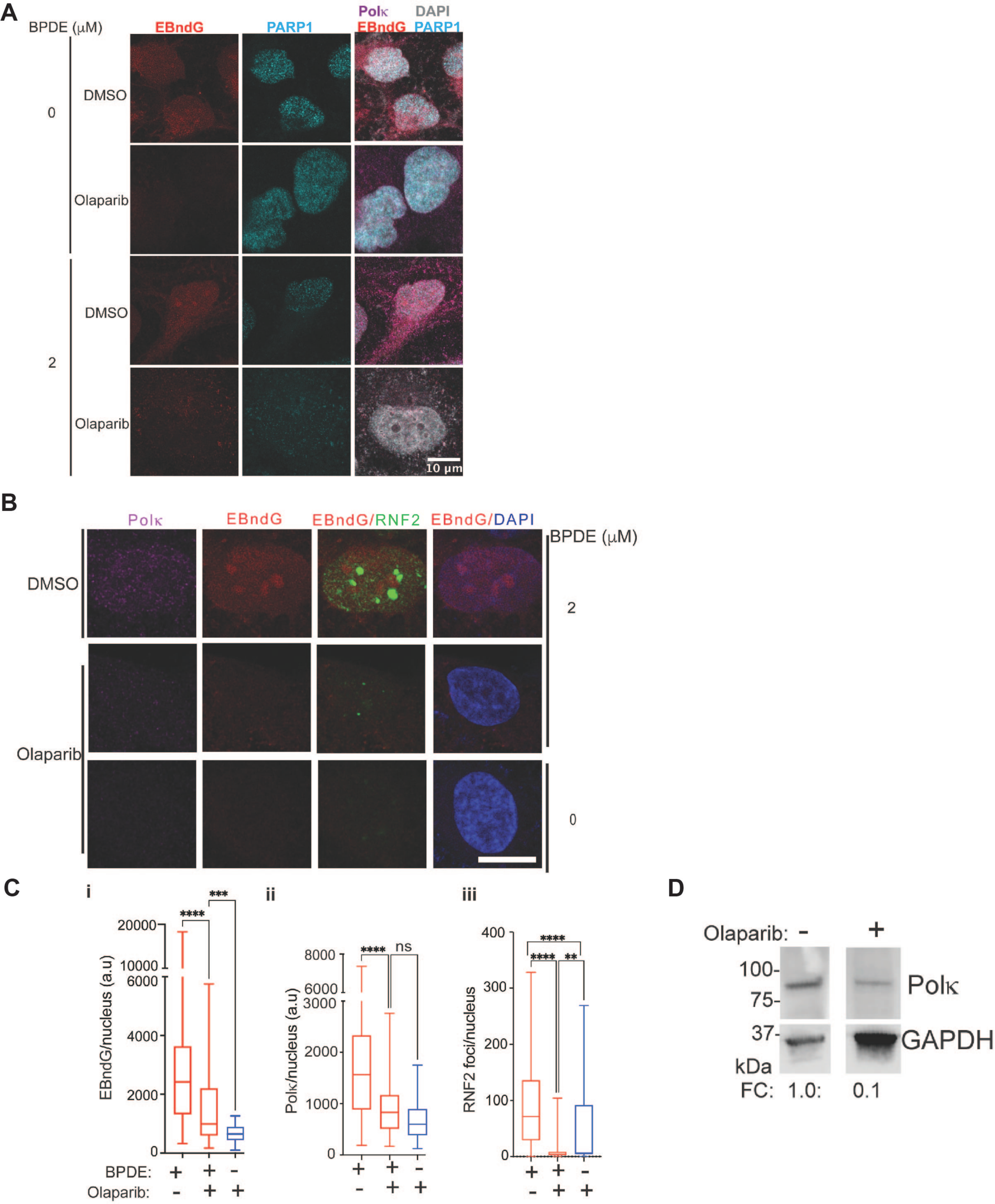
A
BPDE (μM)
EBndG
PARP1
Polκ EBndG
DAPI PARP1
0
DMSO
Olaparib
2
DMSO
Olaparib
10 μm
B
Polκ
EBndG
EBndG/RNF2
EBndG/DAPI
BPDE (μM)
DMSO
2
Olaparib
0
C
i
ii
iii
EBndG/nucleus (a.u)
Polκ/nucleus (a.u)
RNF2 foci/nucleus
BPDE:
Olaparib:
D
Olaparib: - +
100-
75-
37-
kDa
Polκ
GAPDH
FC: 1.0: 0.1

FIGURE 5

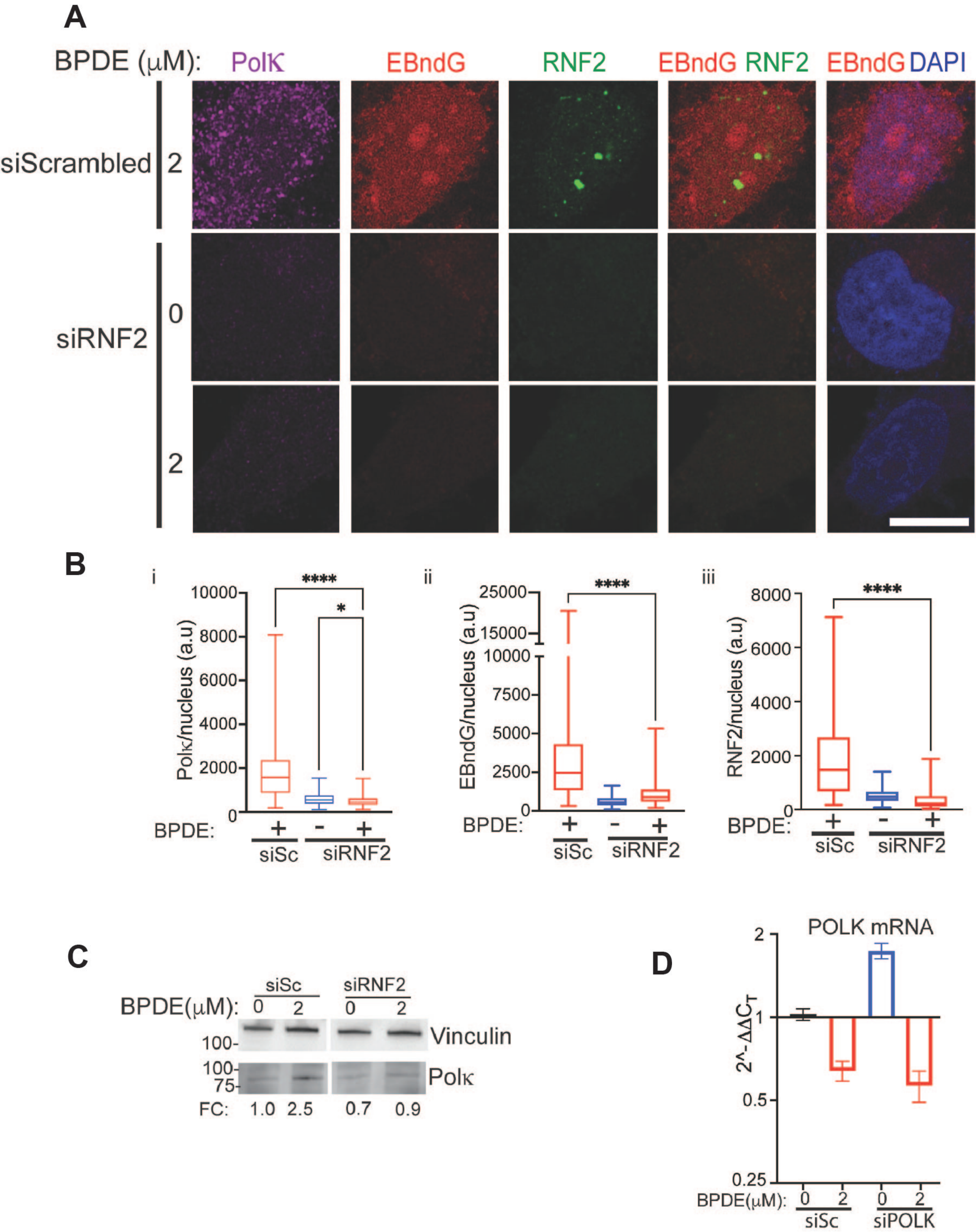
A
BPDE (μM):
PolK
EBndG
RNF2
EBndG RNF2
EBndG DAPI
siScrambled
2
siRNF2
0
2
B
i
****
*
Polκ/nucleus (a.u)
10000
8000
6000
4000
2000
0
BPDE:
+
-
+
siSc
siRNF2
ii
****
EBndG/nucleus (a.u)
25000
15000
10000
7500
5000
2500
0
BPDE:
+
-
+
siSc
siRNF2
iii
****
RNF2/nucleus (a.u)
8000
6000
4000
2000
0
BPDE:
+
-
+
siSc
siRNF2
C
siSc
siRNF2
BPDE(μM):
0
2
0
2
100-
Vinculin
100-
75-
Polκ
FC:
1.0
2.5
0.7
0.9
D
POLK mRNA
2^-ΔΔC_T
2
1
0.5
0.25
BPDE(μM):
0
2
0
2
siSc
siPOLK

FIGURE 6

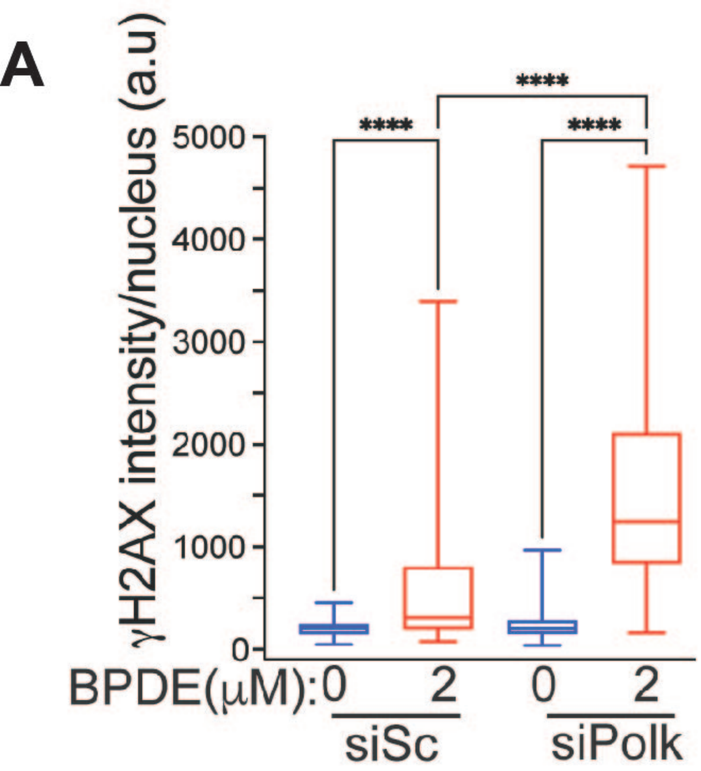
A
γH2AX intensity/nucleus (a.u)
5000
4000
3000
2000
1000
0
****
****
****
BPDE(μM): 0 2 0 2
siSc
siPolk

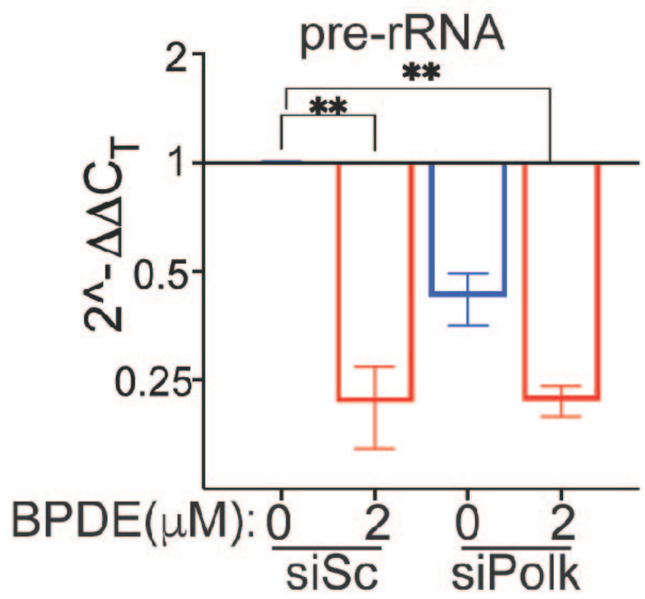
B
pre-rRNA
2^-ΔΔC_T
2
1
0.5
0.25
**
**
BPDE(μM): 0 2 0 2
siSc
siPolk

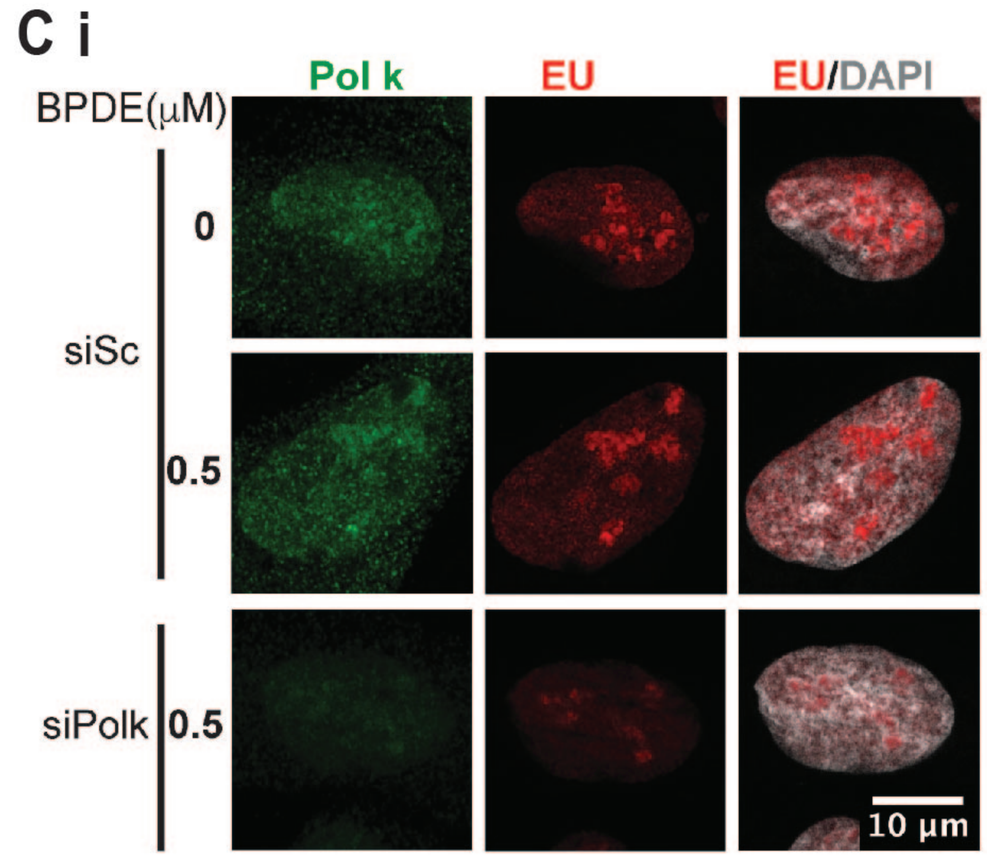
C i
Pol k
EU
EU/DAPI
BPDE(μM)
siSc
0
0.5
siPolk
0.5
10 μm

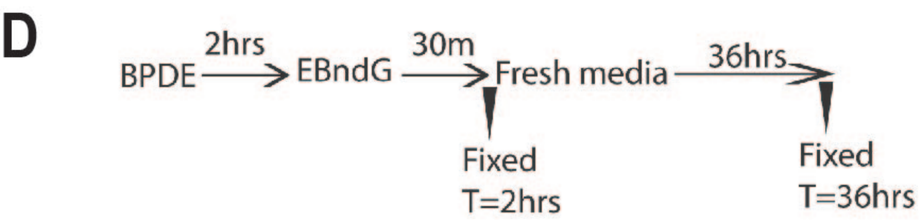
D
BPDE
2hrs
EBndG
30m
Fresh media
36hrs
Fixed
T=2hrs
Fixed
T=36hrs

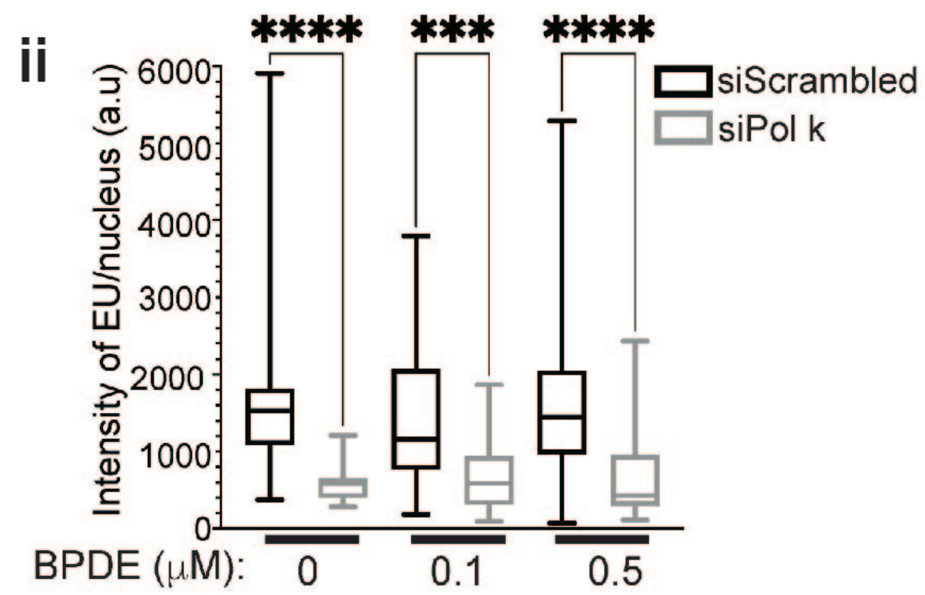
ii
Intensity of EU/nucleus (a.u)
6000
5000
4000
3000
2000
1000
0
****
***
****
siScrambled
siPol k
BPDE (μM): 0 0.1 0.5

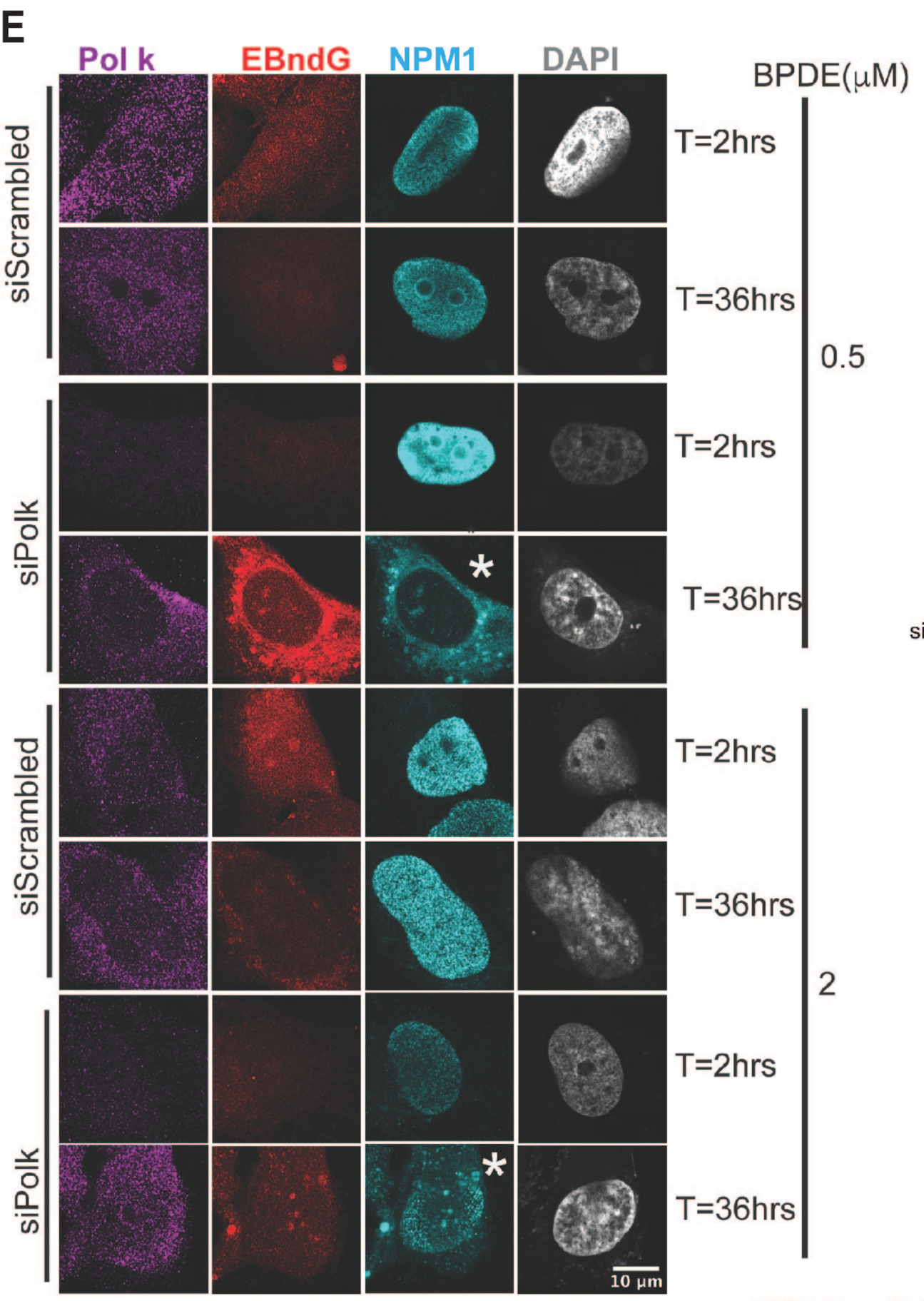
E
Pol k
EBndG
NPM1
DAPI
BPDE(μM)
siScrambled
T=2hrs
T=36hrs
0.5
siPolk
T=2hrs
T=36hrs
siScrambled
T=2hrs
T=36hrs
2
siPolk
T=2hrs
T=36hrs
10 μm

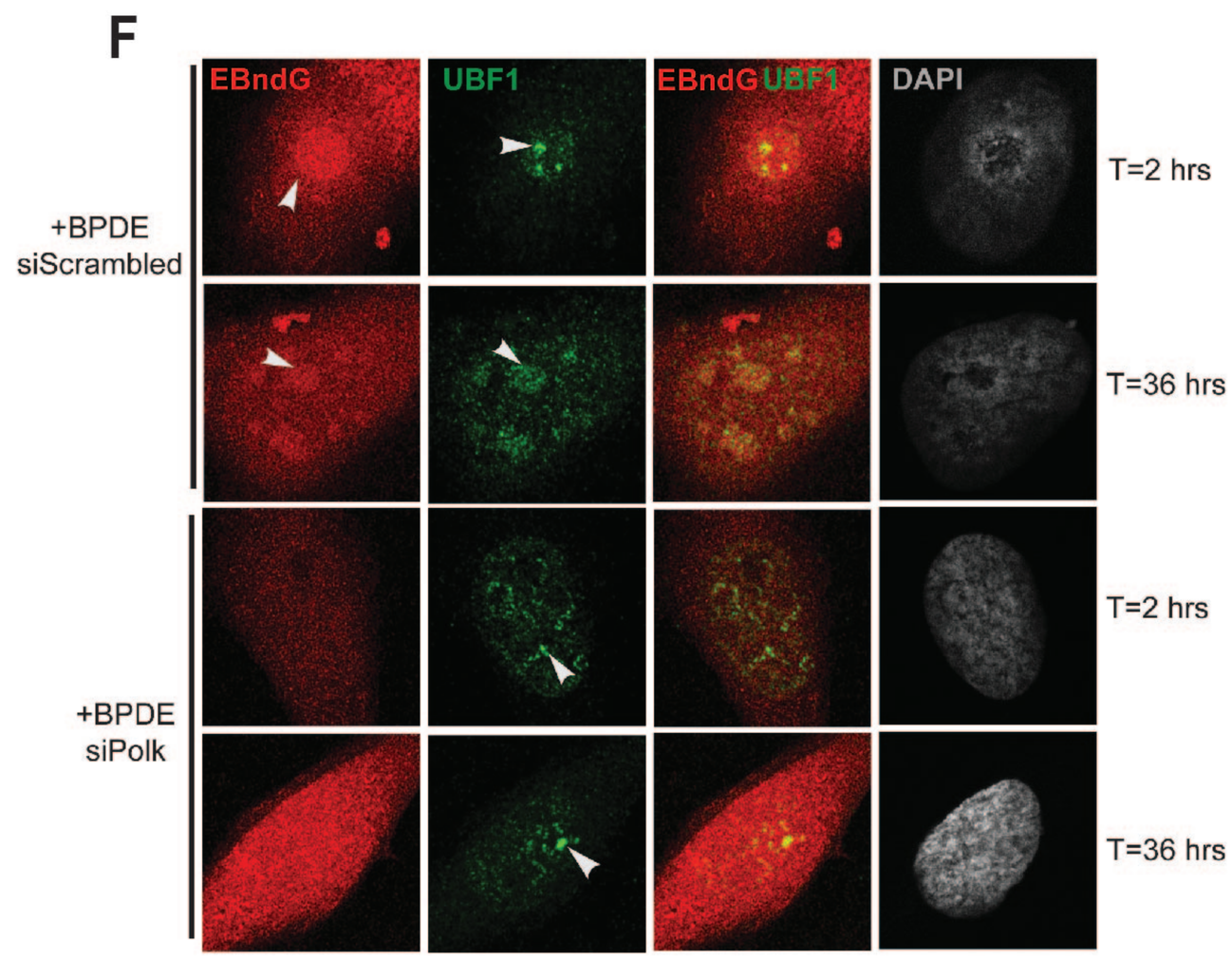
F
EBndG
UBF1
EBndG UBF1
DAPI
+BPDE
siScrambled
T=2 hrs
T=36 hrs
+BPDE
siPolk
T=2 hrs
T=36 hrs

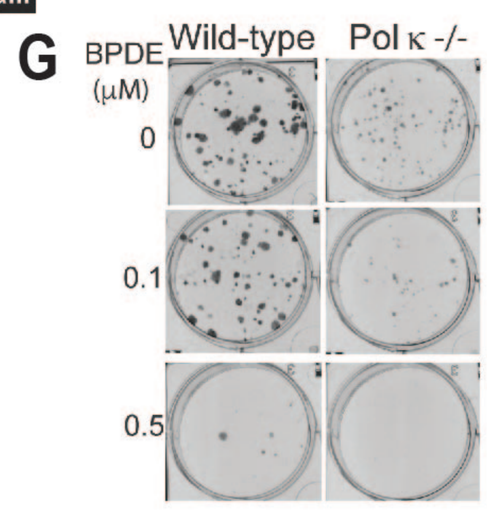
G
BPDE (μM)
Wild-type
Pol κ -/-
0
0.1
0.5

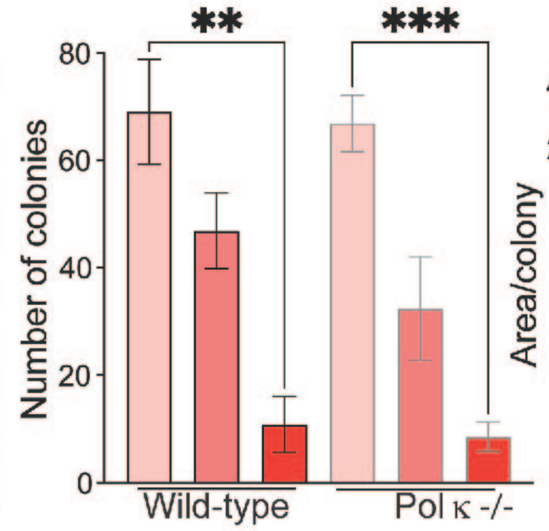
Number of colonies
80
60
40
20
0
**
***
Wild-type
Pol κ -/-

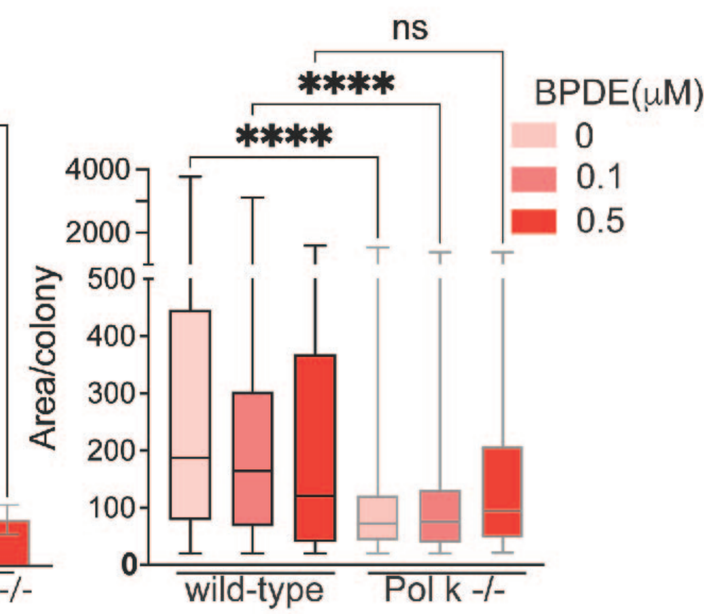
Area/colony
4000
2000
500
400
300
200
100
0
ns
****
****
BPDE(μM)
0
0.1
0.5
wild-type
Pol k -/-

FIGURE 7